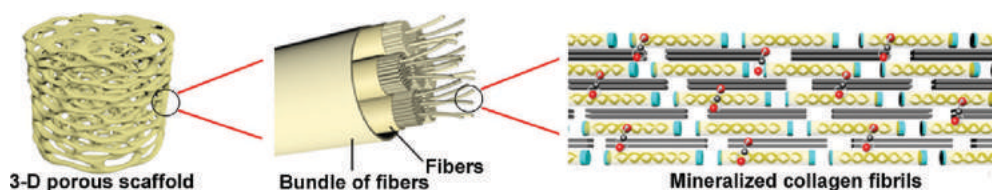


Hierarchical Structures of Bone and Bioinspired Bone Tissue Engineering

Yan Liu, Dan Luo, and Tie Wang*



From the Contents

1. Introduction	2
2. Hierarchical Structures of Bone	2
3. Relationship of Hierarchical Structures and Deformation Mechanism of Bone	6
4. Bone Biomineralization	7
5. In Vitro Models to Explain the Mechanisms of Intrafibrillar Mineralization in Bone	9
6. Synthesis Strategies of Bioinspired CaP Nanocomposites	12
7. Bioinspired Bone Tissue Engineering	15
8. Conclusions and Perspectives	18

Bone, as a mineralized composite of inorganic (mostly carbonated hydroxyapatite) and organic (mainly type I collagen) phases, possesses a unique combination of remarkable strength and toughness. Its excellent mechanical properties are related to its hierarchical structures and precise organization of the inorganic and organic phases at the nanoscale: Nanometer-sized hydroxyapatite crystals periodically deposit within the gap zones of collagen fibrils during bone biomineralization process. This hierarchical arrangement produces nanomechanical heterogeneities, which enable a mechanism for high energy dissipation and resistance to fracture. The excellent mechanical properties integrated with the hierarchical nanostructure of bone have inspired chemists and material scientists to develop biomimetic strategies for artificial bone grafts in tissue engineering (TE). This critical review provides a broad overview of the current mechanisms involved in bone biomineralization, and the relationship between bone hierarchical structures and the deformation mechanism. Our goal in this review is to inspire the application of these principles toward bone TE.

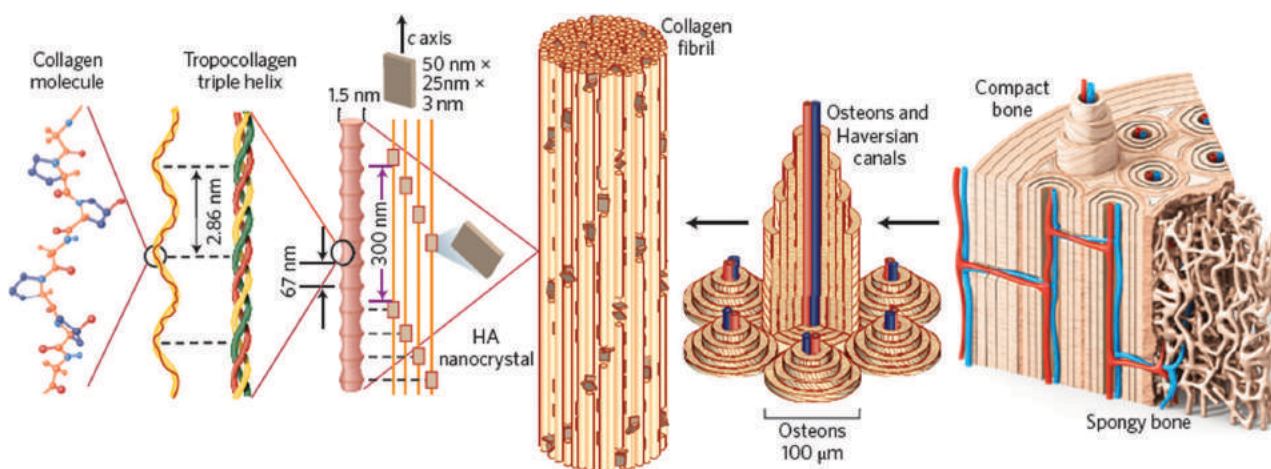


Figure 1. Scheme showing the hierarchical organization of bone from the macro- to the nanoscale. Reproduced with permission.^[1] Copyright 2015, Nature Publishing Group.

1. Introduction

Mineralized biological materials such as bone and sea sponge exoskeletons consist of inorganic and organic phases organized in complex hierarchical architectures, with characteristic dimensions spanning from the nano- to the macroscale.^[1–3] The organic phase plays a crucial role in templating the hierarchical structures of mineralized tissues. The resulting materials often exhibit excellent physical and chemical performances that cannot be achieved by simple combination of their inorganic and organic components. Understanding the complex integration of hard and soft phases involved in natural mineralized tissues is of great value to materials chemistry and provides some useful strategies to synthesize hybrid materials.

Bone consists of cells embedded in extracellular matrix (ECM), which is a hierarchical network made from two major nanophases: Collagen fibrils assembled from type I collagen molecules (ca. 300 nm in length and 1.5 nm in diameter) and hydroxyapatite (HA, $\text{Ca}_{10}(\text{PO}_4)_6(\text{OH})_2$) nanocrystals (plate-shaped, 1.5–4 nm in thickness) deposited along the collagen fibrils.^[4] The self-assembly process of collagen molecules defines the framework and spatial constraints for HA nucleation and propagation.^[5] The HA nanocrystals are principally arranged with their *c*-axes parallel to the collagen fibrils and organized in a periodic, staggered arrangement along the fibrils.^[6–8] This biomineralization process of bone proceeds via a matrix vesicle-mediated mechanism, in which the matrix vesicles are secreted by the outer membranes of bone-forming osteoblasts. The enzyme alkaline phosphatase present in the matrix vesicles cleaves the phosphate esters and acts as the foci for calcium and phosphate deposition.^[9] A large number of non-collagenous proteins (NCPs) are strongly involved in the matrix vesicle-mediated mineralization process.^[9–11] The precise arrangement of the inorganic and organic phases at the nanoscale forms a light-weight, adaptive and multi-functional biomaterial. Like many mineralized tissues, bone derives its fracture resistance from various deformation and toughening mechanisms operating from the nanoscale structure to the macroscopic physiological scale.^[12]

As the primary mechanical support for musculoskeletal locomotion, bone actively remodels throughout the life of a

mammalian organism to maintain skeletal tissue integrity. The study of mammalian bone in a biomineralization and biomimetic context is particularly interesting because the information obtained could have a significant biomedical impact on therapies and strategies to repair or regenerate human mineralized tissues. Our goal in this review is to summarize the current mechanisms involved in the formation of mineralized collagen in natural bone, to reveal the relationship between bone hierarchical structures and the deformation mechanism, and to highlight naturally evolved applications of these principles as an inspiration for engineering. Knowledge acquired in this field may inspire chemists and material scientists to synthesize novel hybrid materials, especially calcium phosphate (CaP) nanocomposites for the regeneration of human bone tissues.

2. Hierarchical Structures of Bone

Natural bone is a heterogeneous and anisotropic nanocomposite, the principal components of which are organized hierarchically into several structural levels, from the macro to the nanometer scale^[1] (**Figures 1 and 2**). The outer geometry

Prof. Y. Liu
Center for Craniofacial Stem Cell Research
and Regeneration
Department of Orthodontics
Peking University School and Hospital
of Stomatology
Beijing 100081, P. R. China

Prof. D. Luo, Prof. T. Wang
Beijing National Laboratory for Molecular Sciences
Key Laboratory of Analytical Chemistry for Living Biosystems
Institute of Chemistry
The Chinese Academy of Sciences
Beijing 100190, P. R. China
E-mail: wangtie@iccas.ac.cn

Prof. D. Luo
State Key Laboratory of Heavy Oil Processing
Institute of New Energy
China University of Petroleum (Beijing)
Beijing 102249, P. R. China

DOI: 10.1002/sml.201600626



and inner architecture of compact/cortical bone and spongy/trabecular represent the macro- and mesoscopic structural levels. Compact bones consist of Haversian canals and osteons. The lowest (nano) hierarchical level features collagen and mineral as the main constituents of the nanocomposite-forming mineralized collagen fibrils, which further assemble into fibers arranged in geometrical patterns in lamellae and osteons. Weiner and Wagner first proposed seven hierarchical levels in the organization of lamellar bone.^[6] Considering the presence of the ordered and disordered materials, Reznikov et al. further divided lamellar bone into nine hierarchical levels (Figure 2).^[13] Although bone structure varies greatly among different locations in the skeleton, the basic building block of bone consisting of mineralized collagen fibrils remains the same throughout.^[6,13] It is the nanostructural level of organization that provides natural bone with its remarkable mechanical properties and remodeling capabilities. Here, we focus on the molecular (level I) and nanostructural (level II) components of bone (Figure 2).

2.1. The Molecular Components of Bone

2.1.1. Collagen Structure

The organic matrix of bone consists of collagen (ca. 90%) stabilized by water and a series of NCPs and lipids. Type I collagen (97%), the most abundant protein present in bone ECM, is synthesized by bone-forming osteoblasts with a highly repetitive amino acid sequence [Gly (glycine)-X-Y]_n, where X and Y are frequently referred to as proline and hydroxyproline residues.^[14,15] This repetitive nature allows three polypeptide chains (two $\alpha 1$ chains and one $\alpha 2$ chain) to fold into unique triple-helical tropocollagen molecules that are ca. 300 nm in length and 1.5 nm in diameter. The tropocollagen molecule is packed into secretory vesicles in the Golgi apparatus and then released into the extracellular space, where the thermodynamic process of collagen fibrils self-assembly is initiated. After the procollagen N-proteinase and the procollagen C-proteinase cleave the C-propeptides and N-propeptides, five tropocollagen molecules self-assemble into a microfibril with the help of inter-molecular hydrophobic and electrostatic forces in a quarter-staggered fashion forming a 67-nm periodicity (D-period) along the molecular axis, a 40-nm gap or hole between the ends of the molecules and a 27-nm overlap region (Figure 3).^[16–19] Figure 3 illustrates the location of a series of charged amino acids that comprise 12 bands of the collagen D-period. These bands are identified and marked as $\alpha 3$, $\alpha 2$, $\alpha 1$, e2, e1, d and c3 (within the hole zone) and c2, c1, b2, b1 and $\alpha 4$ (within the overlap zone).^[19,20] The gap zones are aligned to form thin (ca. 1.5 nm thick) extended slots (called grooves) in which the intrafibrillar crystals appear to grow and nucleate.^[21–23] Microfibrils can aggregate both laterally and longitudinally with other microfibrils in turn to form fibrils whose diameters vary in bone (ca. 100 nm) and whose lengths are too long to determine. When collagen is stained with heavy metal salts, a pattern of alternating dark and light bands perpendicular to the fibril axis could be observed by the transmission electron microscopy (TEM); these bands



Yan Liu is an associate professor at the Department of Orthodontics, Peking University School and Hospital of Stomatology. She studied as a joint-PhD student (2009–2010) at Department of Oral Biology, Georgia Regents University; worked with Prof. Franklin Tay and focused on biomineralization. She received her PhD degree from Huazhong University of Science and Technology in 2011. She joined the faculty at Peking University School and Hospital of Stomatology in 2011. Her research now focuses on biomineralization and bioinspired nanocomposites.



Dan Luo earned his BSc (2008) and PhD (2013) degrees at Peking University Health Science Center. He worked as an assistant professor (2013) at Institute of Chemistry, Chinese Academy of Sciences, and then transferred to China University of Petroleum (Beijing) at 2015. His research focuses on synthesis and self-assembly of high quality nanomaterials.



Tie Wang is a professor at Institute of Chemistry, Chinese Academy of Sciences (ICCAS). He received his BSc (2002) from Xi'an Jiaotong University and PhD (2007) degree from Changchun Institute of Applied Chemistry, China. He worked as a postdoctoral fellow at Rensselaer Polytechnic Institute, Troy, NY, and at University of Florida, Gainesville, FL. He joined the faculty at ICCAS in 2013. His research focuses on the nanoparticle assemblies and their applications.

correspond to the different negatively and positively charged domains.^[24,25] The charged amino acids are expected to play an important role in bone biomineralization.

Collagen, the richest protein in the body, provides mechanical toughness. The alteration of collagen substructural properties is a significant factor contributing to the reduced mechanical properties of bone in ageing and disease. Mutations in the collagen molecular structure by the COL1A1 gene (encoding the $\alpha 1(I)$ tropocollagen chain) are strongly correlated with osteoporosis-related fractures.^[26–28] Furthermore, dysfunctional synthesis of three $\alpha 1(I)$ chains in osteogenesis results in imperfections during formation of a homotrimer of $\alpha 1$ helices, instead of heterotrimers (two $\alpha 1$ chains and one $\alpha 2$ chain), which leads to an altered collagen structure, impaired bone mechanical properties and a more disorganized distribution of mineral apatites.^[28–30]

2.1.2. Mineral Phase

To mineralize bone, bone-forming osteoblasts secrete vesicles containing alkaline phosphatase, which cleaves the phosphate

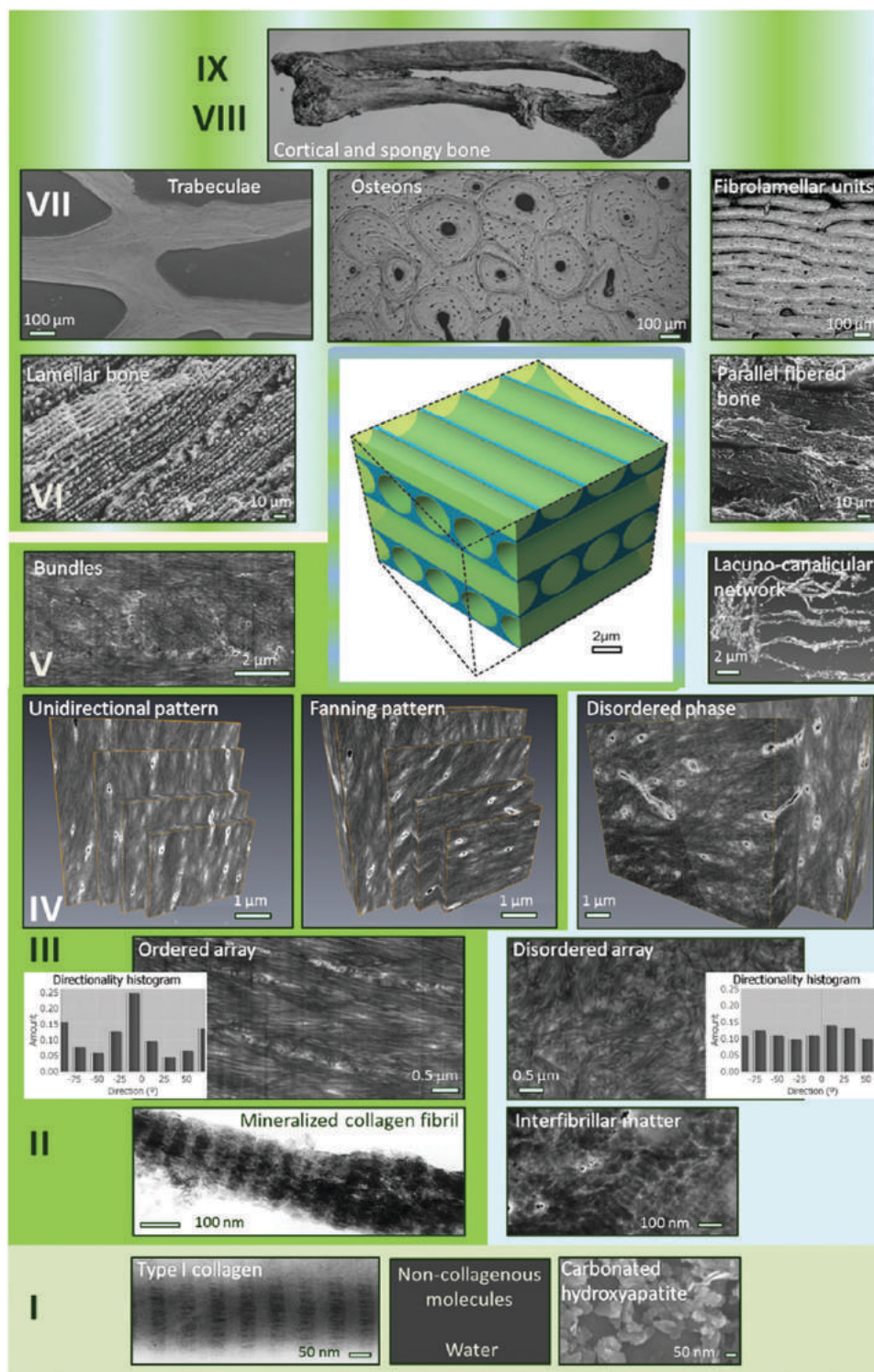


Figure 2. Representative TEM images of the different hierarchical levels of bone. The borders of the images are color-coded: green for the ordered material, blue for the disordered material and a graded color scale where both materials are present. Reproduced with permission.^[13] Copyright 2014, Acta Materialia Inc. Published by Elsevier Ltd.

groups and acts as the foci for calcium and phosphate precipitation.^[9] Bone mineral is mainly composed of HA with a Ca/P ratio of less than 1.67 and contributes to bone stiffness. Natural HA contains impurities such as carbonate (4–6%), sodium (0.9%) and magnesium (0.5%) ions as replacement groups in phosphate and hydroxyl sites, resulting in poorly

crystalline, calcium-deficient and carbonated HA.^[31,32] During the entire process of biomineralization in vivo, the mineral content shows a pronounced local variation and increases from low to intermediate and full mineralization.^[30] The mineral phase of bone, as the stiff and brittle reinforcement of the collagen matrix, strongly influences the stiffness

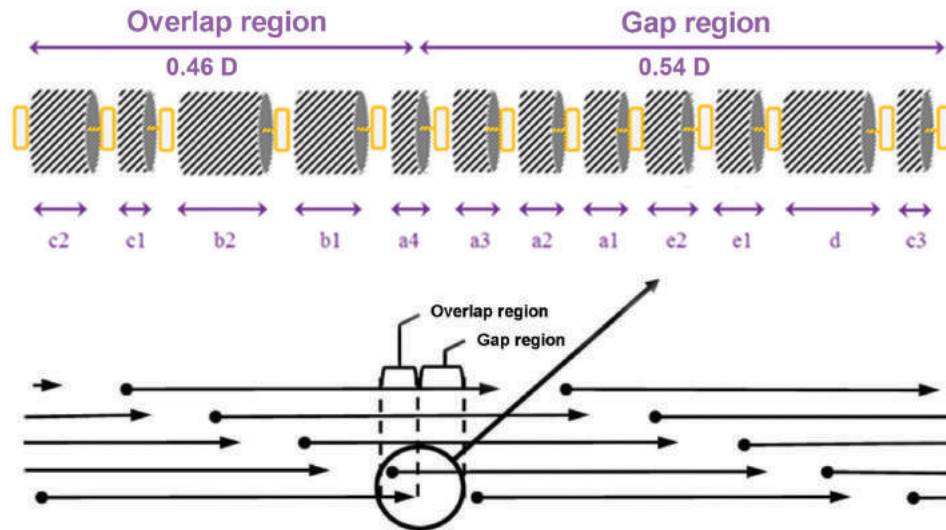


Figure 3. Two-dimensional model of the microfibrillar packing pattern of collagen molecules. Five collagen molecules comprise a microfibril with D-period equal to 67 nm. Twelve bands are identified in the gap (a3, a2, a1, e2, e1, d and c3) and overlap (c2, c1, b2, b1 and a4) zones. Reproduced with permission.^[29] Copyright 2005, Royal Society of Chemistry. Reproduced with permission.^[20] Copyright 2014, Elsevier Ltd.

and breaking strain of bone: A more highly-mineralized bone matrix is stiffer but breaks earlier.^[33,34]

Regarding the morphology of bone HA crystals, there has been much debate on platelets *vs.* needles. The majority of studies describe HA as plate-like, as evidenced by TEM^[35,36] and small angle X-ray scattering (SAXS).^[37–40] One possible reason for the needle-like appearance is that the side-on view of the HA crystals has the strongest absorption contrast in the TEM. In bone, the size of HA crystals varies with thickness ranging from 2–10 nm, length from 20–50 nm, and width from 15–30 nm.^[11,29,32,41] This is partly because of the location of the crystals within the collagen fibrils (smaller) or between collagen fibrils (larger),^[42] and the type of mineralized tissue (e.g., animal species or mature mineralized tissue). Bone mineral is dynamic and is continually being resorbed and built anew during bone remodeling. The small size and/or non-stoichiometry of the HA crystals presumably offers the mineral phase with the solubility required for bone resorption by osteoclasts.^[9] Changes in the shape and size of the HA crystals affect bone strength.^[43]

2.1.3. NCPs

NCPs make up ca.10% of the organic matrix and appear to be critical for regulating mineral nucleation and growth in bone biomineralization.^[44,45] The primary amino acid sequence of NCPs often contains a high density of aspartic acid and glutamic acid residues, which have a high affinity for calcium ions because of their charged carboxyl groups.^[11] The NCPs comprise the small integrin-binding ligand N-glycosylation (SIBLING) proteins and non-SIBLING proteins. The SIBLING proteins, the major group of NCPs, contain dentin matrix protein1 (DMP1, 37- and 57-kD fragments), osteopontin (OPN, 66 kD) and bone sialoprotein (BSP, 75 kD).^[46–48] These proteins are acidic and highly phosphorylated, and play crucial roles in the mineralization of bone and other collagenous tissues.^[22,44,49] The non-SIBLING

proteins contain osteocalcin (OC, 6 kD), which is one of the richest NCPs in bone and is secreted exclusively by osteoblasts; osteonectin (ON, 40 kD), which can interact with calcium ions.^[48]

NCPs exhibit multifunctional roles in bone that are crucial for determining the structural hierarchy and mechanical properties of bone.^[50–53] The removal of NCPs, such as BSP, OC and ON, in knockout mouse models results in alteration of bone geometry and reduction of bone mass and subsequently damages the mechanical properties of bone. Recent evidence suggests that NCPs such as OPN, BSP and OC can serve as “glue” at the collagen-apatite interface to restrain the disassociation of the mineralized collagen and consequently enhance the toughness and stiffness of bone,^[51–53] as well as synthetic nanocomposites.^[54,55]

2.1.4. Water

Apart from the mineral (65 wt%) and organic (25 wt%) phases, water (10 wt%) is the third main constituent of bone.^[32] Liquid water is present in the collagen channels in both unmineralized and mineralized bone, and contributes to the structural and mechanical properties of bone.^[56,57] At level I, water molecules existing between the collagen molecules are responsible for the decreased spacing of these molecules after dehydration. The mineralized lamellae contract less in the orthogonal direction than in the direction perpendicular to the lamellar boundary upon drying (Figure 2).^[13] Dehydration decreases the spacing between collagen molecules, increases the elastic modulus and strength of collagen, and consequently reduces bone toughness. Water molecules stabilize the collagen structure, bridging adjacent molecules through hydrogen bonds. There is also evidence showing hydrogen bonding with water molecules on the surfaces of the bone apatites.^[58–60] The presence of water within defect sites in the HA lattice^[61] might suggest the important role of hydration layers in mineral formation.^[62] Furthermore, water,

as an interfacial agent between collagen and apatite, plays a structuring role in bone biomineralization. It could orient apatite crystals through an amorphous calcium phosphate (ACP)-like layer that coats the crystalline core of bone apatites.^[63] Recently, Xu et al. showed that water localized within the collagen might have a crucial importance on CaP nucleation in intrafibrillar mineralization.^[20]

2.2. Nanostructural Components

The second hierarchical level of bone is formed by the mineralization of collagen fibrils. The mineralized collagen fibril of ca. 100 nm in diameter constitutes the basic building block of the bone biomaterial (Figure 2).^[4,6] Gao et al. proposed a self-similar hierarchical composite material with multi-levels of self-similar structures mimicking the staggered nanostructure of bone.^[64] In their model, every higher level of structure was similar to the nanoscale level of bone (i.e., mineralized collagen fibril). Bone is a platelet-reinforced fibril nanocomposite that contains parallel plate-like HA crystals with their *c*-axes aligned with the long axis of the fibril.^[6–8] This orientation of mineral crystals results in higher strength and stiffness of bone along its longitudinal axis.^[11,30] The nucleation and growth of mineral apatites starts in the gap zones and then partially extends into the overlap zones, forming aggregates of staggered plate-like motifs.^[35,38,65] The mechanism of the formation of mineralized collagen is discussed in detail in Section 5.

3. Relationship of Hierarchical Structures and Deformation Mechanism of Bone

Structural hierarchy is a prevailing feature that can be observed in many biological systems such as bone. The hierarchical structures of bone provide various interfaces from the millimeter to the nanometer scale following the order: Osteon (ca. 100 μm), lamella (ca. 5 μm), fiber bundle (ca. 1 μm), mineralized fibril (ca. 100 nm) and nanophases (collagen molecules and mineral particles).^[66] The propagation of cracks always leads to destruction of materials. However, the unique structural hierarchy of bone, dispersing the deformation energy, enables bone to avoid accumulation of microcracks and prevent further failure. There is a close correlation between orientation for crack propagation and various types of interfaces. In the outer bone shell, cracks propagate along the longitudinal cement line, which is the interface between osteons.^[66,67] The longitudinal and transverse modulus ratio can be expressed in a simplified formula^[68]:

$$\frac{P_L}{P_T} = \frac{P_{ip}}{P_{op}} V_m (1 - V_m) \quad (1)$$

where P_{ip}/P_{op} is the modulus ratio between the inorganic and organic phases and V_m is the volume fraction of mineral. The longitudinal modulus is much higher than the transverse modulus; therefore, deformation occurs parallel to the

longitudinal direction. The driving force for crack propagation in the transverse orientation is five-times higher than that in the longitudinal direction. The interfaces maintained by weak forces will be sacrificed and locally broken during tensile deformation to dissipate energy. The maximum stress sustained by materials with cracks can be calculated using the Griffith equation^[68]:

$$\sigma_{\max} = \sqrt{\frac{2\gamma_s E}{\pi a}} = \frac{YK_{Ic}}{\sqrt{\pi a}} \quad (2)$$

where γ_s is the damage energy, E is the Young's modulus, a is the length of the crack and Y is the geometric parameter. The fracture toughness (K_{Ic}), representing the ability to resist crack propagation, can be determined by the following equation:

$$K_{Ic} = Y^{-1} \sqrt{2\gamma_s E} \quad (3)$$

Within the bone nanostructure, HA nanocrystals and mineralized collagen fibrils behave as reinforcements. Moreover, mineralized collagen fibrils, the basic building block of bone, play an important role in energy dissipation and fracture resistance. This behavior may be attributed to their nanoscale hierarchical structures that combine the tough inorganic HA crystals with the flexible collagen fibrils. The deformation mechanism involving the delicate deformation of mineralized fibrils can be studied by in situ tensile testing. Gupta et al. obtained quantitative data for hydrated bovine parallel-fibered bone through this technique, analyzing the SAXS pattern from high-brilliance synchrotron radiation.^[52] The SAXS patterns were used to analyze the fibril strain under applied stress: the HA nanocrystals were uniformly distributed in the gap regions of the fibrils with a spacing of ca. 0.46D. The gap zone moved apart once the deformation occurred, which resulted in changes in distance that were reflected in the SAXS pattern. The fibril strains and the elastic/inelastic transition points were plotted based on this technique. Additionally, the SAXS data of five equidistant points with an interval spacing of 1 mm along the sample were obtained. These data proved that fibril strain was spatially homogeneous within the sample. The author inferred from a nanometer-level model that the interfibrillar matrix played a crucial role; this matrix is composed of proteins and protein-polysaccharide complexes. The tensile strain is influenced by both tensile stretching of the mineralized fibrils and interfacial shear deformation of the interfibrillar matrix. Microcracks emerged once the bone stretched beyond the critical interfacial shear strength between the collagen fibril and the interfibrillar matrix. The later work of Gupta et al. further clarified the hierarchy of the deformation mechanism at the nanoscale through in situ tensile testing of fibrolamellar bone using synchrotron radiation SAXS/wide-angle X-ray diffraction measurements.^[69] A correlation was found between the strain and hierarchical levels of nanocomposites wherein the strains continuously declined at the tissue, fibril and mineral particle levels at the ratio of 12:5:2. The fracture load with HA nanoparticles (0.15–0.20%) was about double that for bulk HA (0.10%),

which was attributed to the insensitivity of the nanostructured materials to defects. The high strain ratio between stiff HA nanoparticles and ductile collagen fibril translates to a huge difference in mechanical properties, which is beneficial to load transfer at the HA/collagen and fibril/interfibrillar matrix interface.

The mechanical characteristics of mineralized collagen fibrils at the molecular level have been further elaborated through theoretical and analytical models. Although various models have been proposed by different groups to calculate the tissue modulus, these models invariably correlated the modulus and the hierarchical levels of the materials. The longitudinal modulus can be calculated according to the Halpin–Tsai model^[70]:

$$E = E_m \frac{1 + AB\varnothing}{1 - B\varnothing} \times A = 2\rho, \quad (4)$$

$$B = \frac{\left(\frac{E_p}{E_m} - 1\right)}{\left(\frac{E_p}{E_m} + A\right)} \quad (5)$$

where E_m means matrix modulus; \varnothing is the mineral volume fraction; ρ is the percentage of mineral, E_p refers to mineral modulus.

According to Gao et al., the modulus can be estimated as follows^[64]:

$$\frac{1}{E} = \frac{4(1-\varnothing)}{G_p\varnothing^2\rho^2} + \frac{1}{E_{mg}\varnothing} \quad (6)$$

where G_p is the shear modulus of collagen (0.03 GPa); ρ is the aspect ratio of mineral (ca. 30 for bone) and E_{mg} is mineral elastic-modulus (100 GPa).

The modulus can also be written in terms of strains:^[71]

$$E_T \approx (1-\varnothing)E_C \frac{\varepsilon_F}{\varepsilon_T} + \varnothing E_M \frac{\varepsilon_M}{\varepsilon_T} + E_{cf} \quad (7)$$

where E_M and E_C refers to tensile moduli of mineral and collagen phases, respectively, in the mineralized fibril; $\frac{\varepsilon_F}{\varepsilon_T}$ is the fibril-to-tissue strain ratio, $\frac{\varepsilon_M}{\varepsilon_T}$ is mineral to tissue strain ratio and E_{cf} is the tensile modulus of the interfibrillar matrix.

Buehler et al. used a molecular dynamics simulation in a simplified two-dimensional model to analyze the molecular mechanisms of collagen and HA crystals under a large deformation of mineralized collagen fibrils.^[72] Their results indicated that mineralized collagen fibrils could tolerate several hundred micrometers of deformation without leading to macroscopic failure of the tissue. Follow-up work provided details of the deformation mechanism from a three-dimensional, full-atomistic mineralized fibril model, as well as experimental results that compared collagen fibrils with different mineralization levels.^[73] The computer-simulated mineralization process was based on a geometric argument, i.e., HA nucleation and growth in the voids between packed collagen

molecules. The simulated dimension of HA nanoplatelets ($15 \times 3 \times 1.6 \text{ nm}^3$) in the gap region of mineralized collagen fibril with 40% mineral density was in good agreement with the experimental results. Compared with pure collagen fibrils, the presence of HA crystals altered the deformation mechanism under the accumulation of external load: the overlap region exhibited more deformation than the gap region in mineralized fibrils, while deformation of the gap region was more pronounced in pure collagen. The hydrogen bonds and salt bridges between HA and collagen molecules in the gap region of mineralized fibrils benefit load transfer. The stress and strain distributions in mineralized fibrils were further estimated: The inorganic phase could accommodate four times as much stress as the organic collagen phase; nevertheless, the strain in the collagen was two orders of magnitude higher than that in the HA crystals. The complementary distribution of stress and strain between HA and collagen aids energy dissipation and fracture resistance in bone. Qin et al. further investigated the influence of the HA–collagen interface on the deformation mechanism.^[74] The enhancement of the tensile modulus of mineralized fibril was accompanied by increased thickness of HA nanocrystals until the critical size of HA (ca. 2 nm) was reached. The continual thickening of the HA did not increase the tensile modulus, but did increase the brittleness of the HA–collagen composites. The presence of water led to a more consistent relationship between the thickness and tensile modulus or tensile strength of HAs having different chemical surface compositions.

4. Bone Biomineralization

Bone formation occurs biologically by intramembranous ossification and endochondral ossification depending on the type of bone. Intramembranous ossification is common in the development of the skull and other flat bones. This process involves the direct differentiation of mesenchymal progenitor cells into bone-forming osteoblasts; while in endochondral ossification (i.e., primary bone formation), the progenitor cells form an intermediate cartilaginous template that is later rapidly mineralized.^[31,75] The mineralization produces a disorganized “woven” bone microstructure, in which the collagen fibrils are too narrow (10–20 nm in diameter) for the mineral to precipitate within them, thereby resulting in extrafibrillar mineralization.^[76,77] During development or after a fracture, the primary woven bone is gradually replaced by slower-growing lamellar bone (i.e., secondary bone formation) with highly-ordered collagen fibrils (ca. 100 nm in diameter).^[77] Direct organization of the mineral apatites within them results in intrafibrillar mineralization of collagen (IMC).^[78,79] The resulting structure is an ordered mineral–collagen composite with several levels of hierarchy (Figures 1 and 2).

Although bone structure is reasonably well defined, its mineralization remains an enigma. Numerous models have been proposed to describe the complex process of collagen mineralization, but none has completely captured all of the known information. Controversies among researchers still exist regarding the mechanism of mineralization, the

existence of amorphous precursors and the role of matrix proteins. These aspects are reviewed in the following section.

4.1. Transient Precursor Strategy in Bone Biomineralization

The mechanism of the initiation of bone biomineralization remains controversial.^[80] The transient precursor strategy for the initiation of biological apatite formation has been gradually adopted in the biomineralization community because apatite formation does not proceed directly by the association of ions from solution.^[81] Amorphous calcium phosphate (ACP) and/or octacalcium phosphate (OCP) intermediate have been suggested as precursor pathways to biological apatite formation.

The structure of OCP contains hydrogen phosphates and water layers within apatite-like layers, which may account for the observed plate-like crystals in natural bone.^[82,83] Recently, OCP-like phosphate ions have been identified in early intramembranous bone mineral by Raman spectroscopy.^[84] These data might suggest that OCP is the precursor for biological apatite formation. However, the OCP-precursor theory is still not widely accepted because of a lack of compelling and irrefutable structural *in vivo* evidence.

Evidence is accumulating for the ACP-precursor theory in biological apatite formation. Using improved methods of imaging and structure determination such as high-resolution TEM and cryo-TEM, an abundant transient ACP phase has been identified in the formation of apatite crystals in newly formed bones and teeth (Figure 4).^[85–87] Biomineralization of biogenic calcium carbonate in sea urchin spines and spicules also begins with the formation of transient

amorphous precursors.^[88–90] The ACP-precursor theory has been further confirmed by *in vitro* studies, which offered direct evidence of transformation of ACP into apatite crystals.^[32,91–94] The amorphous precursor formation in calcium-based biominerals is thought to proceed through stable prenucleation clusters that are already present in solution before the development of oriented apatite crystals in both calcium carbonate^[95,96] and CaP^[97,98] (Figure 5). Habraken et al. recently revealed that CaP prenucleation clusters are calcium triphosphate complexes that can aggregate into branched three-dimensional polymeric structures from which nucleation of ACP takes place through the simultaneous binding of calcium to form ca. 1.2-nm postnucleation clusters and their aggregation and precipitation as spherical particles.^[99]

4.2. Role of NCPs in Bone Biomineralization

A wide range of NCPs, identified at the mineralizing boundaries of bone, are expected to play essential roles in the regulation of bone biomineralization, such as by initiating ACP formation, apatite nucleation and crystal growth, as well as by inhibition.^[11,44] The SIBLINGs are acidic phosphoproteins that show site-specific binding to collagen molecules and have a capacity to interact with or accumulate calcium ions in their vicinity.^[44] He et al. found that the acidic domains of DMP1 initiated ACP nanoparticles and regulated the phase transition from calcium ACP to carbonated HA.^[45,100] DMP1 also has been shown to serve as a template for apatite nucleation and growth within the gap zones of collagen fibrils^[44,100] (Figure 6). Acidic amino acids in OPN phosphopeptides appear to contribute to HA-inhibiting activity by

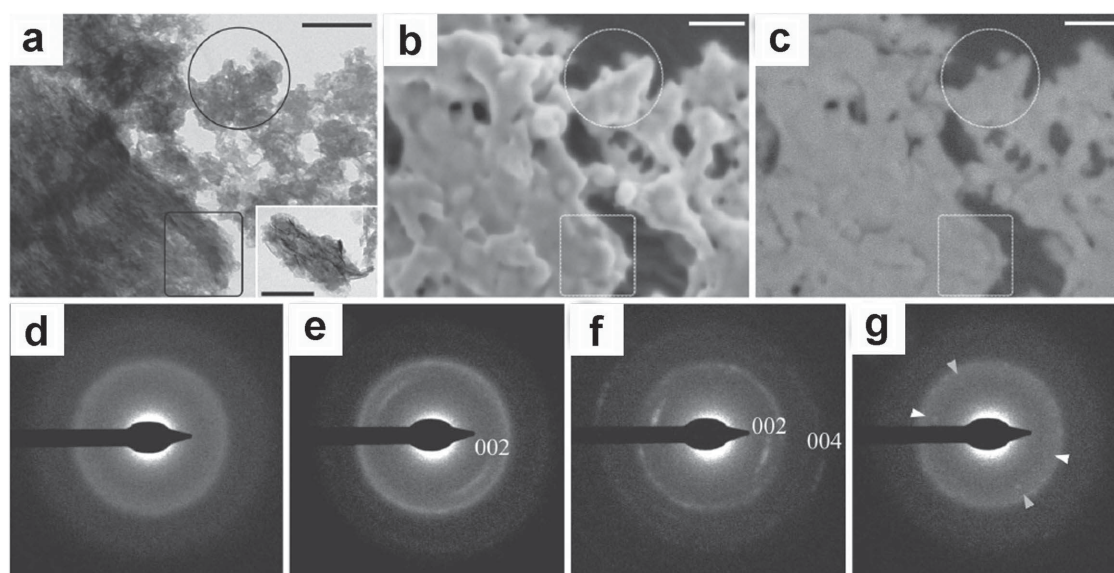


Figure 4. a–c) TEM, high-resolution cryo-scanning electron microscopy (SEM) and energy-selective backscattered images of mineral particle aggregates. d) Corresponding selected area electron diffraction (SAED) pattern of the encircled particle in panel a), showing amorphous scatter of diffuse rings. e) Corresponding SAED pattern of the rectangle in panel a), showing poorly crystalline diffraction. f) Corresponding SAED pattern of the particle in the inset, showing a clearly crystalline diffraction pattern. g) Corresponding SAED pattern of the encircled area examined after storage for 1 week at room temperature. Scale bars = 100 nm. Reproduced with permission.^[85] Copyright 2008, National Academy of Sciences, USA.

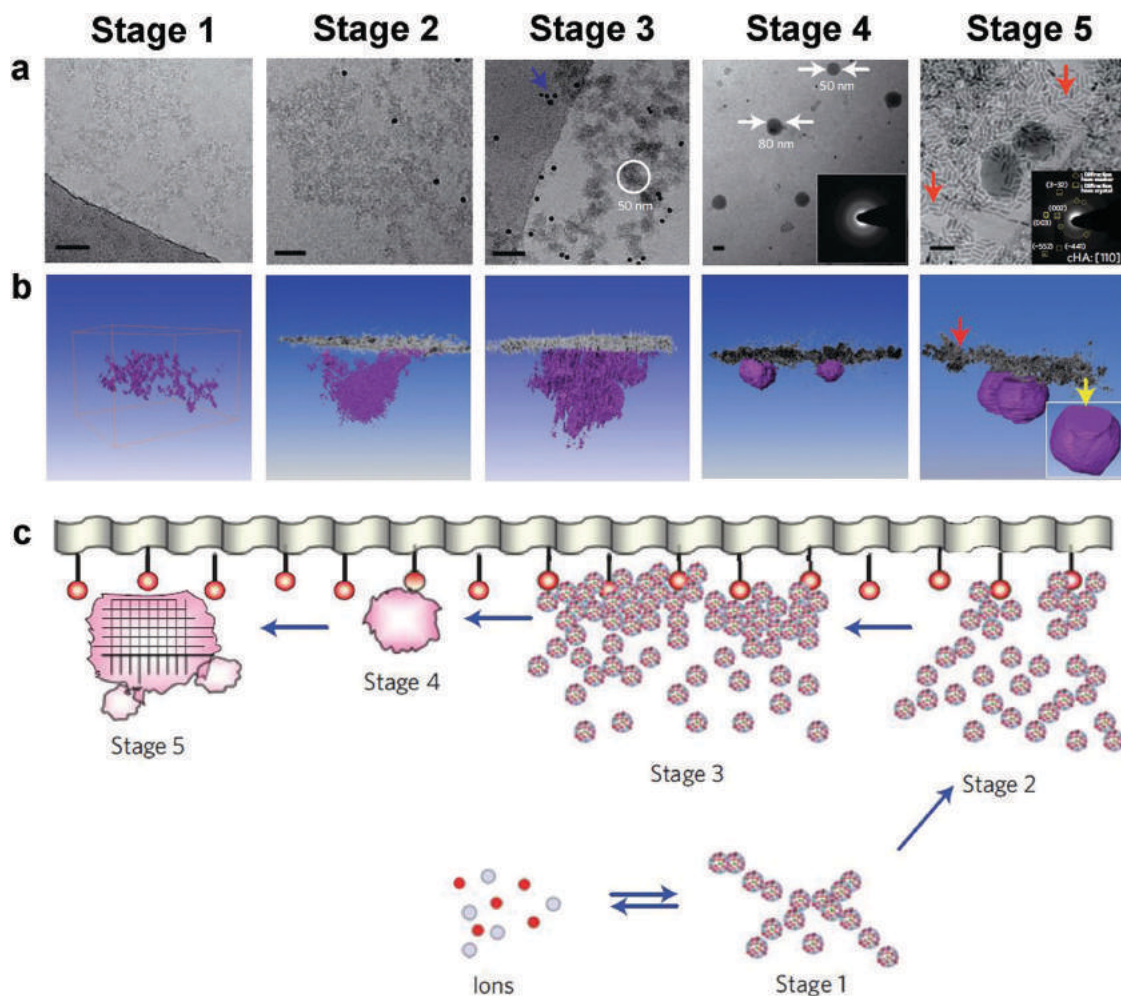


Figure 5. a) Two-dimensional cryo-TEM images of different stages of surface-induced apatite nucleation from simulated bodyfluid. Scale bar = 50 nm. b) Computer-aided three-dimensional visualizations of tomograms. The inset SAED at stage 4 shows that the spherical particles attached to the monolayer are amorphous. The inset SAED at stage 5 can be indexed as carbonated hydroxyapatite (HA) with a $[110]$ zone axis. c) Scheme of the mineralization process in panel a). Reproduced with permission.^[97] Copyright 2010, Nature Publishing Group.

producing an electrostatic repulsion of inorganic phosphate ions once the protein is adsorbed to the crystal surface. However, BSP facilitates HA nucleation when immobilized on the collagen fibrils. Furthermore, the mineralization effect of BSP is closely correlated with acidic, glutamate-rich peptide sequences.^[101]

Functional motifs within the NCPs are particularly important for mineralization. Phosphatases such as enzyme alkaline phosphatase^[9] and PHOSPHO1,^[102] which is highly expressed within matrix vesicles, play a critical role in the initiation of mineral formation.^[9,103] Phosphorylation of NCPs is essential for apatite nucleation and growth within collagen fibrils.^[100] The phosphorylation level of OPN regulates the inhibition or nucleation of HA.^[104,105] A recent study compared the effect of phosphorylated vs. non-phosphorylated DMP1 on collagen mineralization and showed that the former facilitated highly organized IMC (**Figure 7**). Conversely, the use of non-phosphorylated DMP1 resulted in randomly oriented intrafibrillar crystallites, with no particular orientation of their crystallographic axes with the longitudinal axis of the collagen fibrils.^[49]

5. In Vitro Models to Explain the Mechanisms of Intrafibrillar Mineralization in Bone

Vertebrate mineralized connective tissues such as bones possess unique mechanical properties that are required to resist various stresses and forces. These properties derive from the precise collagen–mineral architecture, in which carbonated HA crystals preferentially deposit inside the gap zones of collagen molecules during the early stages of mineralization and partially extend into the overlap zones of collagen molecules in the later stages of mineralization, forming cross-banding pattern.^[36,106–109] To understand the mechanisms underlying this intrafibrillar mineralization, various in vitro models have been developed, including electrostatic interaction, capillary force and size-exclusion models.

5.1. Electrostatic Interactions

It is generally accepted that vertebrate mineralization occurs in extracellular compartments closely correlated with organic

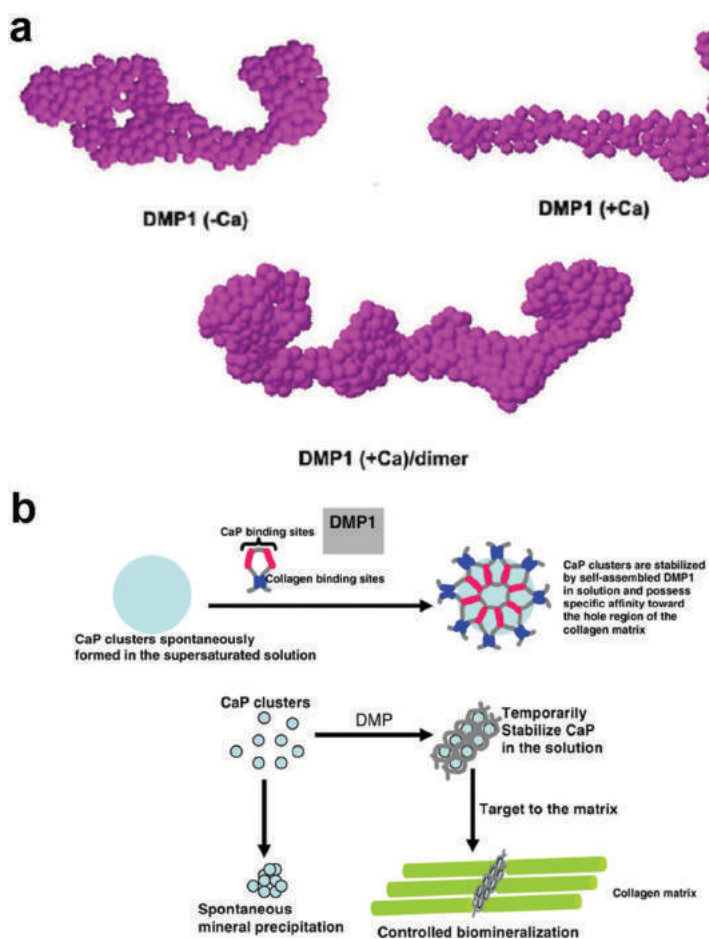


Figure 6. a) Structural analysis of DMP1 in the absence and presence of calcium by the ab initio program GASBOR. b) Proposed model for the dual functional role of DMP1: inhibition of spontaneous mineral precipitation and promotion of controlled mineral nucleation on a collagenous template. Reproduced with permission.^[44] Copyright 2008, American Chemical Society.

matrix components. The multiple electrostatic interactions between charged side chains of associated proteins in ECM and free calcium or phosphate ions may promote nucleation of CaP minerals in vertebrate mineralization.

The functional role of type I collagen in bone biomineralization remains controversial, even after several decades of research. Early studies suggested that there is no direct interaction between collagen and mineral phase. Collagen itself could not initiate biomineralization, but acted as a passive depot for resettlement of apatite crystallites through interactions with NCPs.^[11,110] The acidic NCPs could specifically bind to the gap zones of collagen molecules inducing mineral nucleation inside the collagen fibrils.^[111] Matrix phosphoproteins, as highly-phosphorylated polyanionic macromolecules, could attract calcium ions and serve as templates for nucleation and growth of apatites within the gap zones of collagen fibrils.^[44,91,92,100] During this process, the comparatively loose amorphous structure of ACPs is transformed into a more closely-packed crystalline structure.^[112]

In contrast to the previous studies, type I collagen was recently proposed to take an active role in biomineralization by serving as a template. The electrostatic attractions between collagen

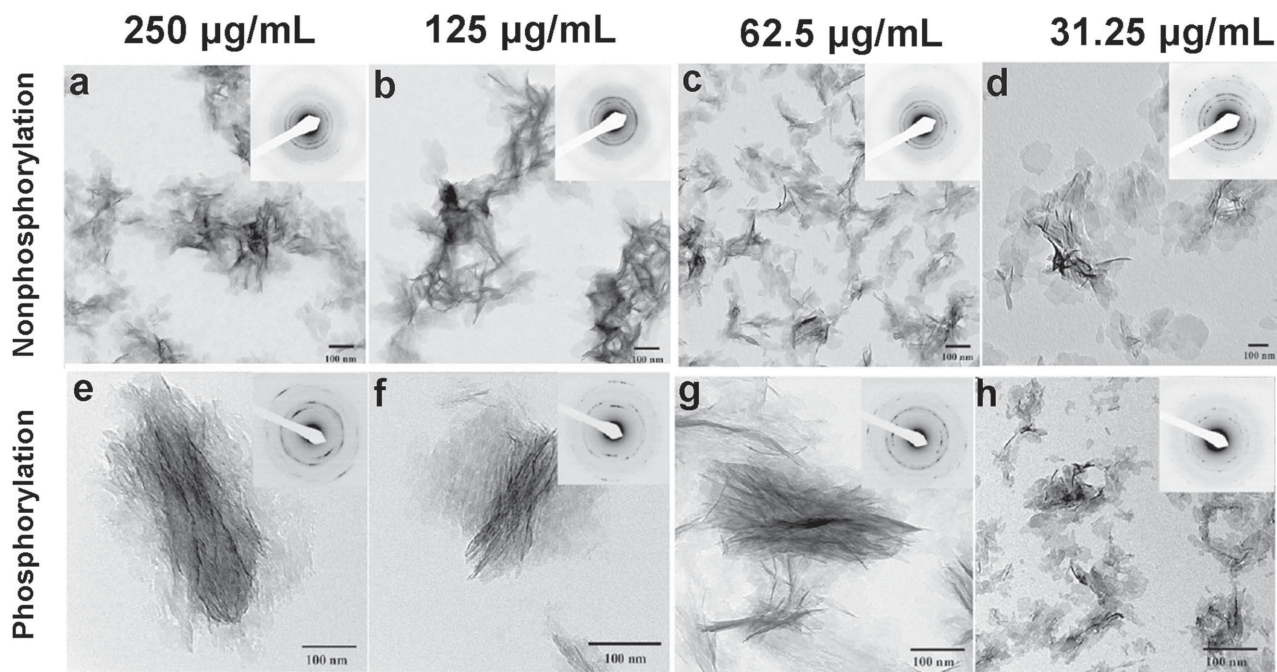


Figure 7. TEM images and corresponding diffraction patterns of crystallites formed in the presence of recombinant nonphosphorylated and phosphorylated DMP1 at different concentrations. Reproduced with permission.^[49] Copyright 2011, American Chemical Society.

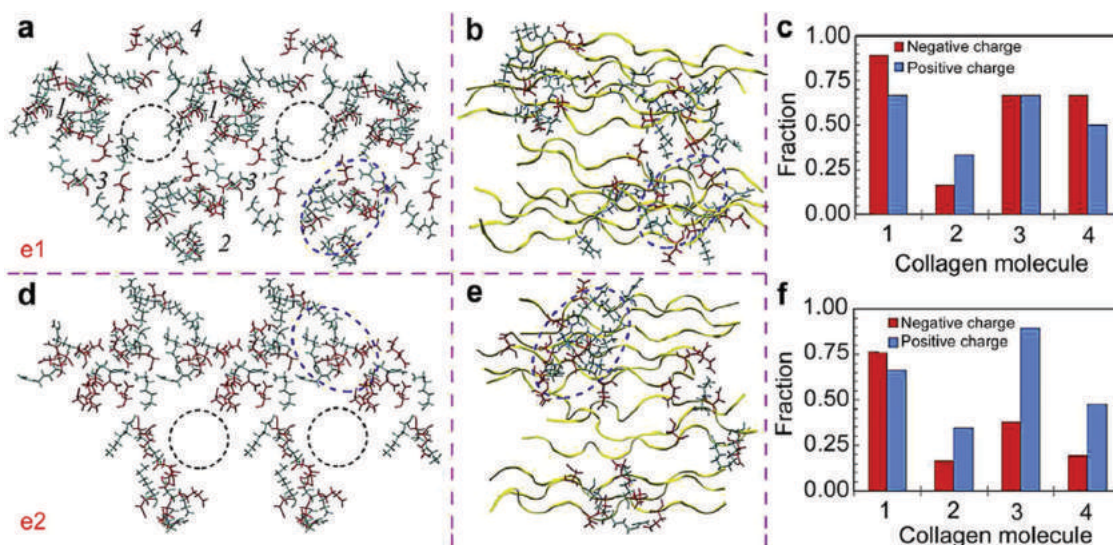


Figure 8. Configurations of charged sidechains around the e1 and e2 bands of the gap zone. a,d) View down the crystallographic *c*-axis. Dashed black circles: gap zones. b,e) View parallel to the crystallographic *c*-axis. Dashed blue ellipses: closely-interacted sidechains. The backbone of the molecules is shown in a yellow ribbon format. c,f) The fraction of charged sidechains pointing into the gap zone for each collagen molecule. The blue color represents positively charged groups; the red color represents negatively charged groups. Reproduced with permission.^[20] Copyright 2014, Elsevier Ltd.

and calcium ions or ACP nanoparticles directly induce apatite deposition within the gap zones. Systematic analysis of the primary amino acid sequence of human type I collagen indicated that collagen molecule is a biomacromolecule rich in charged amino acids and these charged amino acids are thought to be oriented toward the gap zones of collagen molecules.^[23,113] Since the e1 and e2 bands are the earliest mineralization sites *in vivo*,^[23] Xu et al. analyzed the e1 and e2 band structures around the gap zones using molecular dynamics simulations and found that most of these charged sidechains were concentrated at one or two positions along the collagen backbones of the e1 and e2 bands (**Figure 8**).^[20] The charged groups in the e2 band were even more densely distributed than those in the e1 band. The charged sidechains in both bands can potentially sequester and bind calcium ions through electrostatic interactions; thereby templating nucleation of amorphous CaP clusters in the mineralization process. This study confirmed that CaP mineralization proceeds by means of amorphous prenucleation clusters.^[97,98] Based on these findings, type I collagen appears to provide a molecular framework for directing apatite formation without any intervention of other ECM components. In this regard, the *in vitro* simulated experiments also proved that purified collagen molecules promote nucleation of apatite in the absence of any other vertebrate ECM molecules.^[114–116] Wang et al. further revealed that the collagen matrix affects the atomic-scale structural characteristics and controls the size and three-dimensional distribution of apatite.^[116] Moreover, Nudelman et al. enriched this theory that collagen could also attract negatively-charged polyanion-stabilized prenucleation clusters into positively charged regions of collagen fibrils, which further control the apatite nucleation.^[94,98]

5.2. Capillary Force Theory

In contrast to other theories, this model suggests that HA crystals do not initially nucleate within the gap zones, but derive from a liquid-phase amorphous precursor, which can be drawn into the nanoscopic gaps and grooves of collagen fibrils by means of a capillary force. Once the precursor entering into the gap region, solidification and crystallization upon loss of hydration waters subsequently occur to acquire thermodynamically stable phase, resulting in IMC.^[32,117] This theory is based on the hypothesis that the initial mineral phase is transient ACP stabilized by acidic NCPs and the capillary action occurs within an aqueous mineralization solution. A highly specific, epitaxial-type interplay with acidic NCPs is not necessary to promote crystal nucleation and direct crystal orientation.^[111] Instead, collagen fibrils themselves actively regulate the nucleation of oriented crystals.

5.3. Size-Exclusion Theory

The size-exclusion theory proposes that the collagen fibril not only provides the aqueous compartments for mineral growth, but also acts as a gatekeeper in bone biomineralization: proteins with molecular weight smaller than 6 kDa can freely diffuse into the inner spaces of the collagen fibril whereas molecules weight larger than 40 kDa protein are excluded from this water.^[118] In this regard, large-size acidic NCPs inhibit mineralization outside the collagen fibril because NCPs with large dimension are repelled outside the gap zones. Consequently, crystal growth is selectively inhibited everywhere but within the collagen fibril, resulting in initial mineral deposition in the gap zones of the fibril.^[119] Most SIBLING proteins, such as BSP, appear too

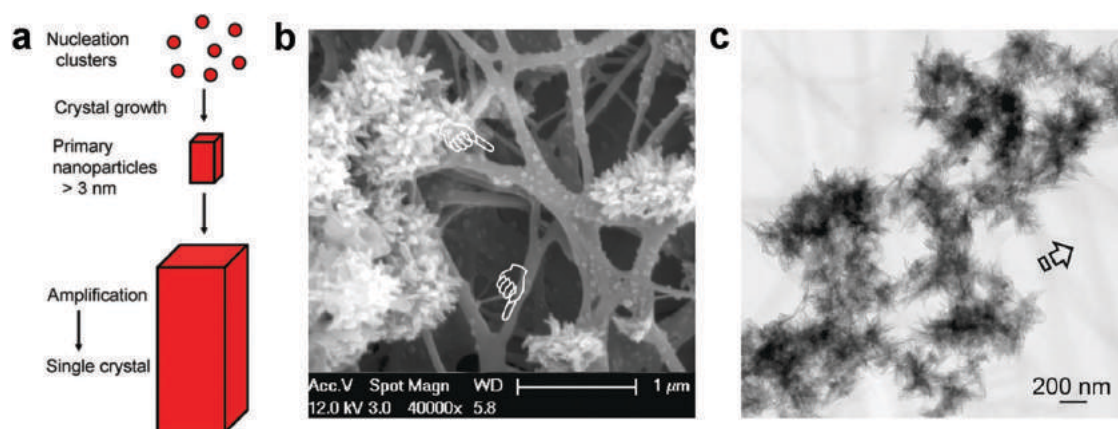


Figure 9. a) Schematic illustration of the classical crystallization theory. b) SEM image of EMC, showing apatite clusters around the collagen matrix. c) Unstained TEM image of EMC. Open arrow: unmineralized collagen. a) Reproduced with permission.^[129] Copyright 2006, Royal Society of Chemistry. b,c) Reproduced with permission.^[135] Copyright 2011, American Chemical Society.

large ($M_w > 40$ kDa) to enter into the collagen fibril and their phosphorylated conformations might extend into interfibrillar spaces, attracting calcium and phosphate ions and leading to apatite nucleation.^[22,120–122] Only single ions and molecules with $M_w < 6$ kDa, such as OC, are considered as small enough to diffuse into the gap regions.^[122] Therefore, BSP and OC, would appear to regulate apatite nucleation and growth in the interfibrillar spaces in bone mineralization *in vivo*, which supports a recent hypothesis of collagen-mediated mineralization.^[22,23]

6. Synthesis Strategies of Bioinspired CaP Nanocomposites

6.1. Classical Ion-Mediated Crystallization Strategy for Bulk CaP Composites

Traditional *in vitro* collagen mineralization strategies often involve the use of metastable calcium and phosphate ion-containing solutions and/or various forms of simulated body fluid as the reaction media.^[123–126] The classical ion-mediated crystallization theory considers nucleation formed by reaction between ions in metastable solution and subsequently grow into larger crystallites. This process starts from clusters generated by primary building blocks like atoms, ions or molecules and grow further via ion-by-ion attachment and unit cell replication.^[127–129] (**Figure 9**). The cited studies primarily reported extrafibrillar mineralization of collagen (EMC), where apatite crystals were randomly oriented on the surface of the collagen fibrils. During this process, the enrichment of calcium cations on the surface of collagen fibrils resulting in formation of spheric clusters and local supersaturation followed by apatite nucleation.^[14,130,131] Although CaP mineral dimension could be successfully controlled by the classical crystallization model, it is difficult to replicate the native bone hierarchical nanostructure generated from intrafibrillar mineralization.^[132] The EMC is limited to its insufficient strength, which makes it not suitable for further application of bone TE.^[133–135]

6.2. Polymer-Induced Liquid-Precursor (PILP) Pathway for Intrafibrillar Mineralization

The contemporary concept of biomineralization has been recently advanced by the identification of non-classical particle- and precursor-based crystallization mechanisms.^[136] Different from the classical ion-mediated crystallization strategy, formation of amorphous precursor phases, instead of nucleation, is considered to be the fundamental step in mineralization.^[88,89] Gower et al. initially proposed the concept of polymer-induced liquid precursor (PILP), which provides a general way for a broad range of crystalline materials to control phase transformation processes.^[117,137] The plasticity of the PILP phase allows it to be portrayed as various non-equilibrium crystalline structures (**Figure 10**).^[117,138,139]

A fundamental breakthrough in simulating the native bone IMC has been developed using the PILP strategy. This strategy proposes that a liquid-phase mineral precursor is infiltrated into the gaps and grooves of the collagen fibrils by means of a capillary force.^[32,117] The adjunction of acidic polymers (i.e., simple analogs of NCPs) to the supersaturated mineralization solution stabilizes a highly-hydrated amorphous precursor and simultaneously delays nucleation and growth of crystals to form a metastable solution.^[32,140–143] The collagen fibrils themselves can actively regulate the nucleation of oriented HA crystals. Recently, OPN, one of the NCPs in bone ECM, was applied in the PILP process, which is similarly served as a process-directing agent for the IMC formation. Moreover, the inclusion of OPN promotes the interaction between osteoclasts and PILP-remineralized bone. These findings suggest that the PILP process may allow for biomimetic bone graft substitutes with bioresorbable property through the cellular processes of bone remodeling.^[144] However, the HA crystals formed in the PILP process are uniformly distributed within the gap and overlap regions of the collagen fibrils, resulting in formation of continuous apatite strands throughout the entire D-period of type I collagen.^[32] Recreating the architecture of IMC from an amorphous precursor is an important step toward reproducing the hierarchical nanostructure of natural bone. This PILP

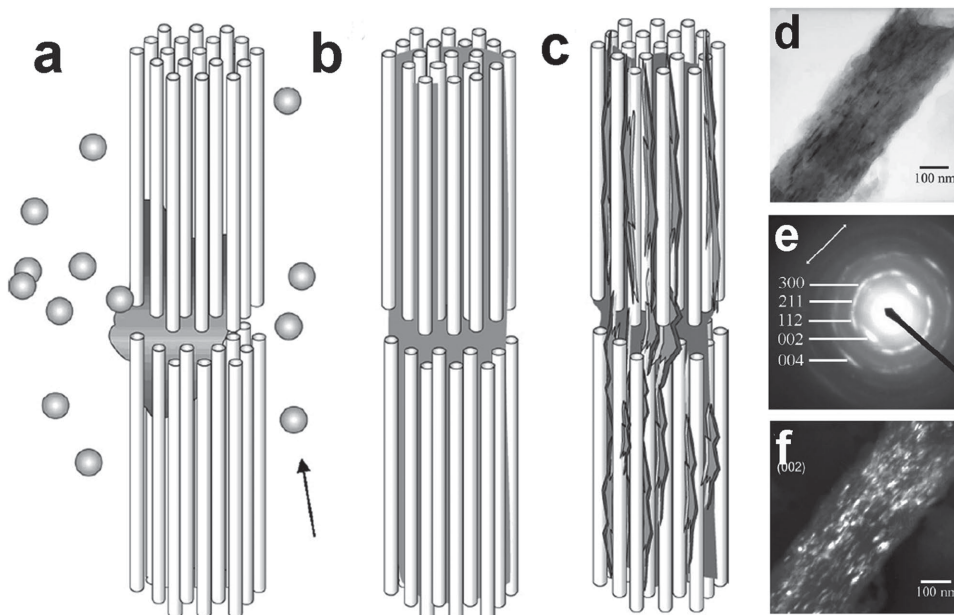


Figure 10. a–c) Schematic illustration of the PILP process. a) Negatively-charged polymer stabilized ACPs (arrow) adsorb to the positively-charged C-propeptide of the collagen fibril. b) ACP nanodroplets infiltrate into the space through the fibril. c) ACPs crystallize forming lamellar HA crystals. d) Bright-field TEM image of a single mineralized fibril mineralized by the PILP process. e) Corresponding SAED pattern of panel d) demonstrates that the mineral phase is HA. f) Dark-field TEM image of the same fibril, using the [002] reflection, shows the prevalence of oriented crystallites within the fibril. Reproduced with permission.^[117] Copyright 2008, American Chemical Society.

strategy, by using acidic polymers alone as an apatite nucleation inhibitor, challenges earlier findings that the phosphorylated conformations of NCPs are strongly involved in the mineralization of collagenous tissues.^[44,49,100]

6.3. Dual Biomimetic Analog-Based Bottom-Up Strategy for Hierarchical Intrafibrillar Mineralization

Inspired by the dual functional role of matrix phosphoproteins in bone biomineralization,^[145,146] Tay et al. pioneered

a dual biomimetic analog-based bottom-up strategy to reproduce the hierarchical organization of apatites in the native bone IMC (**Figure 11**).^[91,92,135,147,148] Polycarboxylic acids such as polyacrylic acid (PAA) or polyaspartic acid were employed as biomimetic NCP analogs for binding and sequestering calcium ions to prevent aggregation of fluidic ACP nanoparticles and auto-transformation of the ACP nanoparticles into apatite before they enter into the intrafibrillar water compartments of the collagen fibril. Additionally, polyphosphates including polyvinylphosphonic acid,

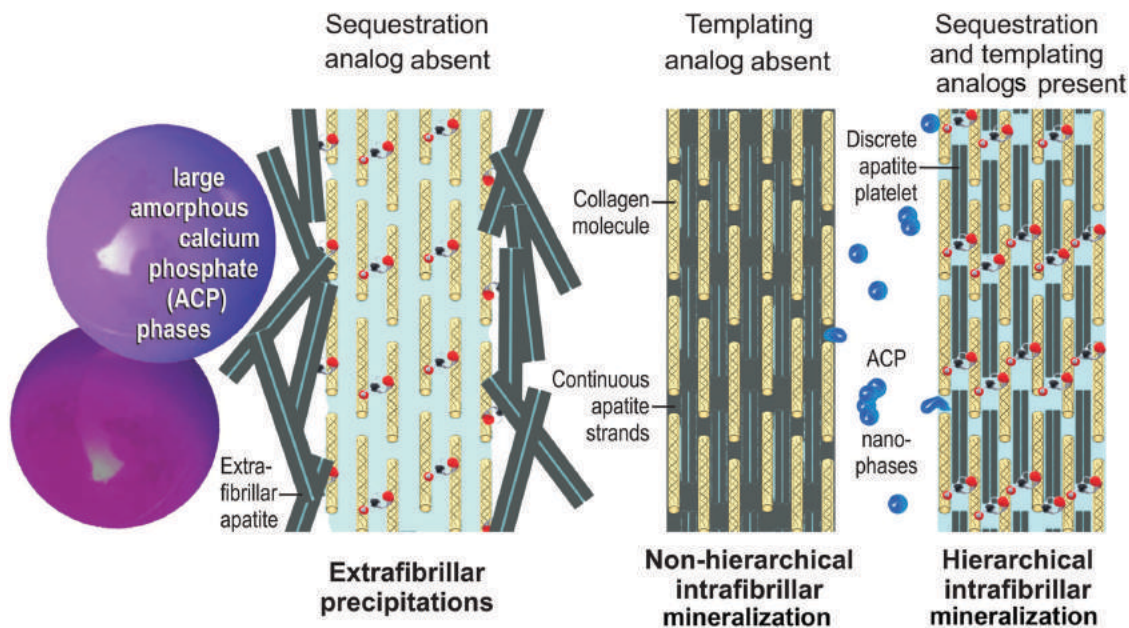


Figure 11. Scheme of different mineralization processes using different combinations of sequestration and templating analogs. Reproduced with permission.^[91] Copyright 2010, Elsevier Ltd.

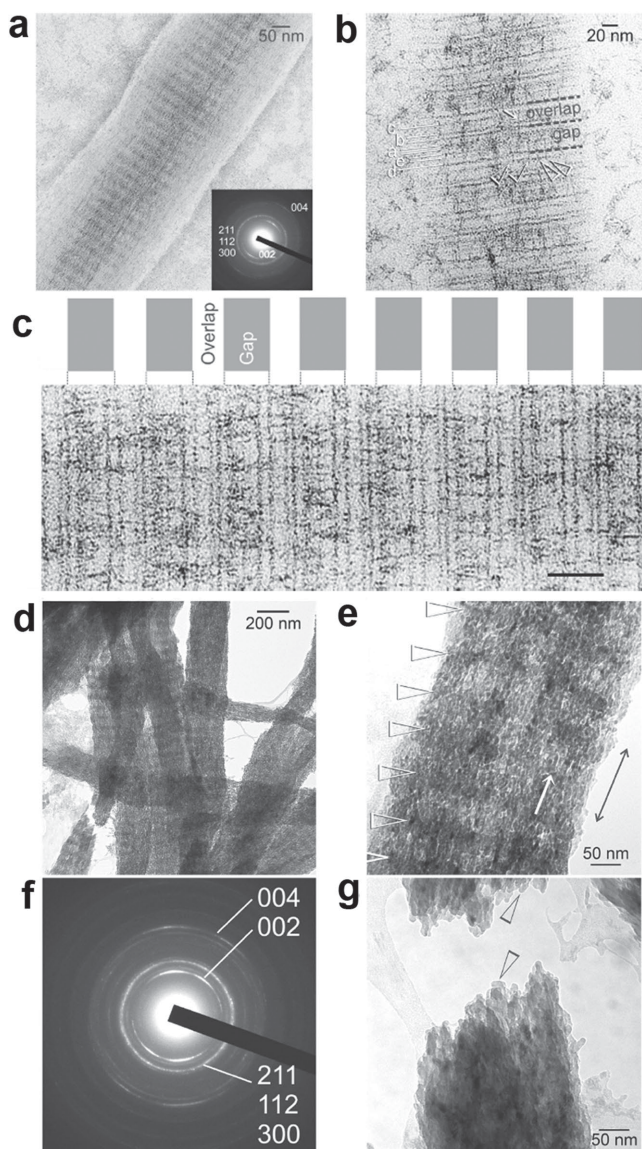


Figure 12. a) Unstained TEM image of the initial stage of periodic apatite arrangement. Inset: SAED reveals poor crystallinity. b) Stained fibril mineralized for 24 h. c) Stained fibril mineralized for 48 h. Scale bar = 50 nm. d) Unstained fibrils mineralized for 72 h. e) High magnification of panel d), showing mineral platelets (arrow) arranged along the long axis of fibril (double arrowhead) resulting in a distinct cross-banding pattern (arrowheads). f) Corresponding SAED pattern of panel e), showing arc-shaped diffraction patterns. g) Fractured fibril indicating intrafibrillar apatite platelets (arrowheads). Reproduced with permission.^[135] Copyright 2011, American Chemical Society.

sodium trimetaphosphate (STMP) and sodium tripolyphosphate (TPP) were used as another biomimetic NCP analog for templating deposition of intrafibrillar apatites. Because self-assembled purified collagen molecules do not comprise bound matrix proteins, a two-dimensional single layer of collagen fibrils was reconstituted and mineralized using this biomimetic bottom-up strategy.^[91,92,135] After 24 h, the apatites with poor crystallinity attached to the D-spacings of collagen fibrils and mainly deposited in the gap zone templated by TPP (**Figure 12a,b**). The deposition of apatites along the gap zone became denser after 48 h, resulting in distinct

cross-banding pattern (**Figure 12c**). After 72 h, the unstained nanocomposites were heavily mineralized with intrafibrillar HA nanoplatelets, which reproduced hierarchical nanostructure of the native bone IMC (**Figure 12d-g**).^[135] Exploiting the basic processes of reconstituted collagen in the context of intrafibrillar mineralization could create opportunities for the design of TE materials for hard tissue repair and regeneration.

Previous studies have shown that IMC can be produced by using poly(aspartic acid) alone as a nucleation inhibitor to stabilize ACP, without the adjunctive use of polyphosphate analogs.^[32,94,149,150] Although this biomimetic mineralization strategy can reduce preparation time of mineralized collagen scaffolds from a TE perspective, this simplified approach can not lead to universal success and ignores the widespread existence of highly phosphorylated NCPs in bone biomineralization. A recent study compared the effect of using single (sequestration) vs. dual (sequestration and templating) biomimetic analogs for mineralization of a two-dimensional single layer of collagen fibrils.^[91] The results showed that IMC with continuous apatite strands instead of cross-banding pattern was acquired by using PAA only as an apatite nucleation inhibitor. Conversely, the adjunctive use of STMP as a templating analog led to IMC with discrete apatite crystallites (**Figure 13**). One reasonable explanation for formation of continuous apatite strands might ascribe to the PILP process mentioned above: the PAA-stabilized ACP nanoparticles infiltrated into the interconnecting water-filled spaces within collagen fibrils and further transformed into continuous single crystalline throughout the gap and overlap regions. Such a crystallization mechanism creates IMC entities similar to the monolithic single-crystal structure of sea urchin spines and siliceous bio-skeletons.^[151,152] Moreover, release of poly(anionic) acid into the intrafibrillar compartments may lead to penetrated swelling and relaxation of the collagen microfibrillar arrangement, which promotes continuous apatite growth extending from the gap zones into overlap zones, and consequently forming continuous strands. Conversely, electrostatic binding of polyphosphates to collagen fibrils may inhibit continuous apatite growth along the overlap zones, thereby confining apatite platelets within the gap zones.^[91] Although the PILP mineralization mechanism is important in an amorphous precursor-based biomineralization system, formation of a continuous single crystal is not what Nature has intended apatite to be precipitated within collagen fibrils in vertebrates for the purpose of bearing loads.^[69]

6.4. Bioinspired Intrafibrillar Mineralization by Poly(amidoamine) Dendrimers

Intrafibrillar mineralization of collagen with bone-like hierarchy can be achieved by the dual analog-based strategy,^[91,92,135,147,148] which involves two different NCP analogs in solution and multiple steps. Therefore, a more facile strategy based on one analog to fulfill dual functional role of NCPs in hierarchical, intrafibrillar mineralization is really desirable. Dendrimer is a kind of mono-dispersed polymer

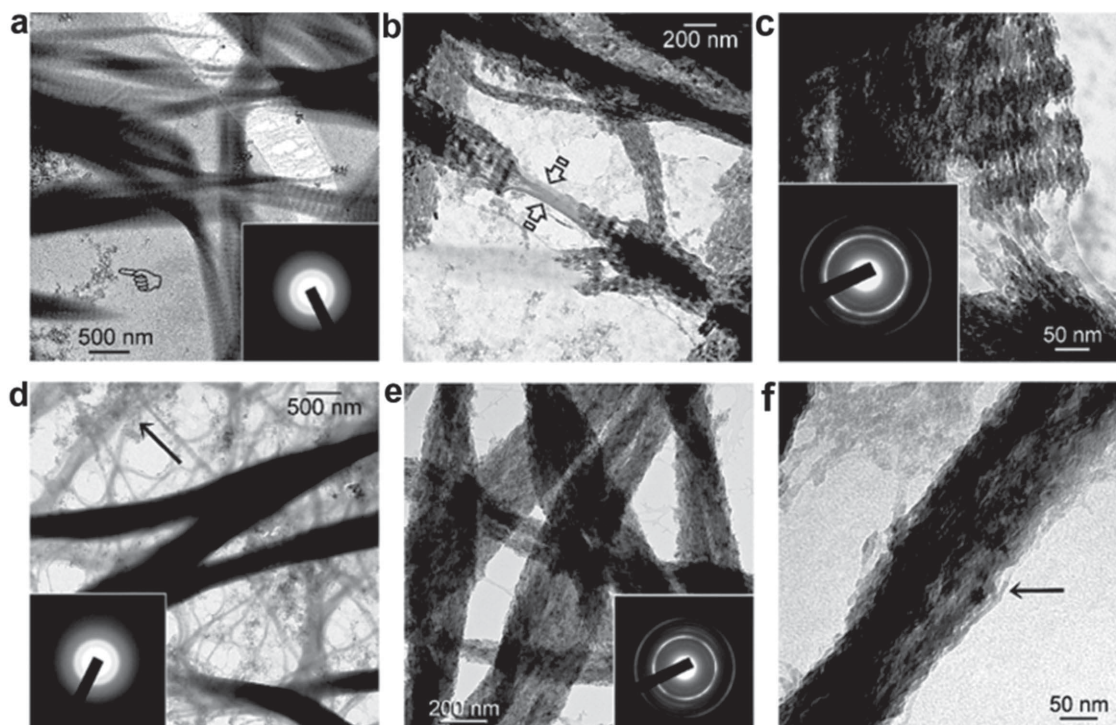


Figure 13. a–c) Unstained TEM scopy images of collagen mineralized in the presence of sequestration and templating analogs. a) 24 h of mineralization, showing cross-banded collagen fibrils containing amorphous electron-dense minerals (inset). b,c) 72 h of mineralization, showing the hierarchical arrangement of overlapping nanoplatelets. Inset: SAED showing ring patterns. d–f) Unstained TEM microscopy images of collagen mineralized in the presence of sequestration analogs only. d) 24 h of mineralization, showing swollen, electron-dense fibrils with a smooth appearance. Inset: SAED showing amorphous mineral phase. e,f) 72 h of mineralization, showing continuity of the mineral strands and absence of cross-banding patterns. Inset: SAED showing ring patterns. Reproduced with permission.^[91] Copyright 2010, Elsevier Ltd.

with highly-ordered/easily tailored architecture (i.e., controllable steric structure and functional group), which makes it as an ideal candidate for NCP analog.^[153] Poly(amido amine) (PAMAM) dendrimer has been widely applied to regulate the size and shape of HA in the biomineralization field.^[154,155] Yang et al. synthesized an amphiphilic PAMAM dendron with a self-assembly behavior similar to amelogenin, which initially aggregated to nanospheres and further translated to linear chains to induce HA mineralization in vitro.^[156] However, free dendrimer in solution has low binding capability to HA and could not obtain in situ regeneration or remineralization. Therefore, Wu et al. conjugated PAMAM dendrimer with alendronate, which could easily adsorb on the surface of HA, and finally induced in situ remineralization of tooth enamel.^[157] They further achieved intrafibrillar mineralization of reconstituted single layer of type I collagen fibrils by using carboxylated PAMAM dendrimer (PAMAM-COOH)^[158] (Figure 14). In that study, the PAMAM-COOH was immobilized on the collagen fibrils via electrostatic interaction and size-exclusion properties ($M_w = 10.1$ kDa), and ACP nanoparticles existed during the initial stage of the remineralization process. This strategy based on one analog to fulfill sequestration and templating functions of NCPs^[159] was much simpler and could realize in situ collagen remineralization. However, the cross-banding pattern of mineralized collagen is not obvious. This may be due to the structure of the reconstituted collagen fibrils, which did not show distinct periodicity (Figure 14a).

7. Bioinspired Bone Tissue Engineering

Bone is a complex and dynamic form of mineralized collagenous tissue that remodels throughout life to adapt to mechanical stress, and maintain ionic balance and skeletal tissue integrity. Bone loss frequently occurs in the following situations: the imbalance between bone formation and resorption that is associated with osteoporosis, large bone deficiencies caused by severe trauma, congenital malformations and surgical resections; therefore alternatives are required to reverse bone defects and regenerate bone.^[160] The bone grafts from autologous (i.e., from a patient's own body) or allogeneic (from another human) sources are widely applied in conventional strategies for bone repairing. However, complications such as donor-site morbidity, limited supply and dimensions, host immune rejection and disease transmission limit their further applications.^[161–163] Bone TE is a rapidly developing discipline to repair, replace or regenerate the lost bone. Investigation the chemical composition and hierarchical micro- and nanostructures of natural bone provide a favorable strategy to reproduce biomimetic artificial bone grafts.

Bioinspired fabrication of bone tissue involves applying principles identified from both bone mineralization processes and bone's structural and mechanical properties. However, incorporating all characters presented in natural bone formation into bone TE is still challenging, since the bone tissue is inherently dynamic and complex. A general goal of

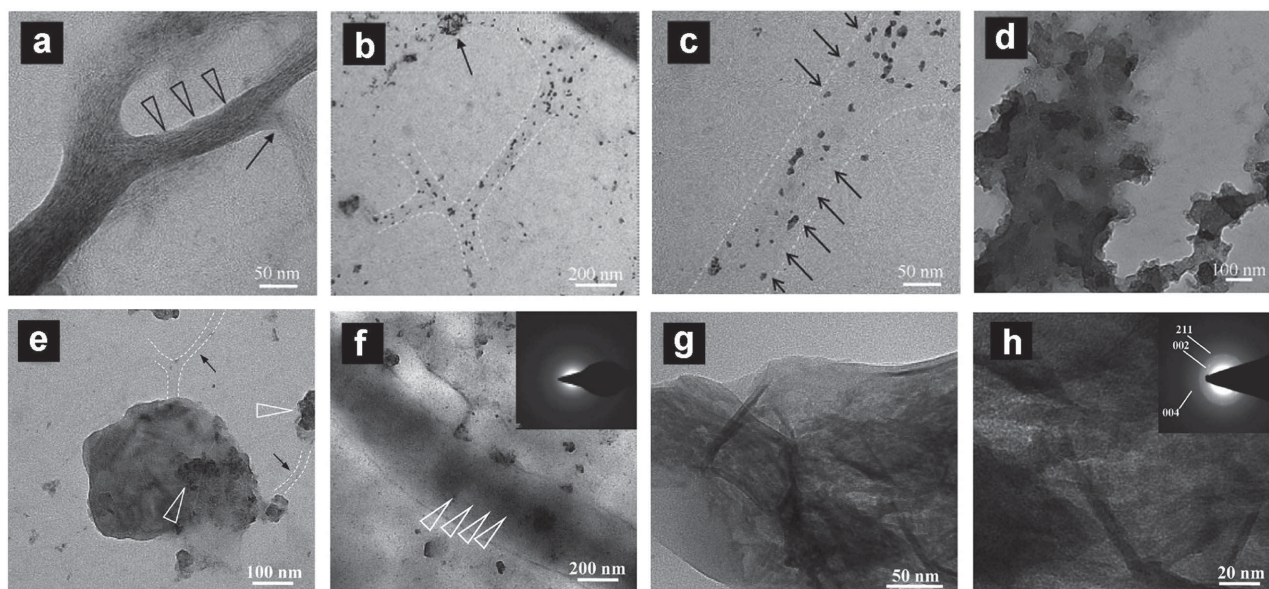


Figure 14. a) Stained TEM image of reconstituted collagen fibrils. b) Unstained collagen fibrils immobilized with PAMAM-COOH and mineralized in artificial saliva for 3 days. c) Magnification of fibrils in panel b). d) Magnification of the coalesced nanoprecursors in panel b) (arrows). e) Unstained collagen fibrils immersed in artificial saliva for 7 days. f) Unstained collagen fibrils immobilized with PAMAM-COOH and mineralized in artificial saliva for 7 days. Inset: SAED of the fibril suggesting an amorphous mineral phase. g) PAMAM-COOH immobilized collagen fibrils mineralized for 14 days. h) Magnification of panel g). Inset: SAED of the fibrils showing apatite mineral phase. Reproduced with permission.^[158] Copyright 2013, Elsevier Ltd.

bioinspired bone TE is to generate bone grafts that: (1) mimic the chemical composition and nanostructure of the bone surface because biocompatibility, surface properties and biodegradation are important aspects of bone-grafting scaffolds; (2) simulate the structural and cell-interactive properties of the bone ECM; (3) provide sufficient initial mechanical strength and stiffness to substitute for lost bone, support proliferation and differentiation of osteoblasts and the expression of bone ECM; and (4) possess a three-dimensional porous interconnected network with adequate mechanical strength for vascular tissue ingrowth.^[164] Since bone ECM is a nanocomposite containing collagen and HA mineral, biomimetic nanocomposites based on collagen and CaPs, and nanofibrous scaffolds with well-defined architectures are selected for discussion as follows.

7.1. Self-Assembly of Collagen Nanofibers

During bone biomineralization process, the self-assembly of collagen fibrils defines the framework and spatial constraints for HA growth. Therefore, the *in vitro* self-assembly and mineralization of collagen have drawn much attention in bone TE. Early studies to reproduce bone ECM focused on using a synchronous collagen biomineralization process, which was initiated by the precipitation of an ACP phase when the self-assembly of collagen fibril began.^[165–167] The ACP phase was then slowly transformed to nanocrystalline HA, which precipitated on the surface of collagen fibrils. The resultant homogenous collagen/CaP nanocomposite could be formed into membrane-like “tapes”, which could induce osteogenic differentiation of human marrow stromal cells^[168,169] and showed degradation rate similar to bone matrix *in vivo*.^[170]

For the application in bone TE, three-dimensional porous collagen/CaP scaffold was further produced by a freeze-drying process, which leads to interconnecting pores with diameters of approximately 200 μm suitable for homogenous cell seeding and new bone ingrowth (**Figure 15**).^[171,172] However, this synchronous collagen biomineralization process neglects the important role of NCPs in HA biomineralization and could not reproduce the nanoscale architecture of native bone, which may result in low compressive strength.

To reproduce a functional, engineered bone tissue with consistency of structural and biological functions, the most important factor is to design scaffolds with nano- and micro-sized architectures similar to those of native bone. Using a modified biomimetic mineralization approach, Liu et al. demonstrated the principle of hierarchical mineralization within a fibril at the molecular and nanoscale levels. The ACP nanodroplets promoted aggregation of microfibrils to form nanofibers; meanwhile, the microfibrils, in turn, templated hierarchical arrangement of nanodroplets in periodically-spaced gap zones or intermolecular spaces.^[93] According to atomic force microscopy (AFM) results, this hierarchical IMC exhibited better mechanical properties compared with pure collagen and EMC (**Figure 16**). This finding was similar to the behavior of natural bone, whose mechanical properties mainly arise from the intrafibrillar apatites within the gap zones of the fibrils.^[7,69,173] Furthermore, the three-dimensional fibrillar matrices of IMC provided excellent biological functions, including initial cell biocompatibility, further cell differentiation and mineralization (**Figure 17**).^[93,174] It is suggested that improved nanomechanics and biological functions could be achieved through simulating a hierarchical architectures of natural bone, which may eventually result in novel biomaterials for bone grafting and TE applications.

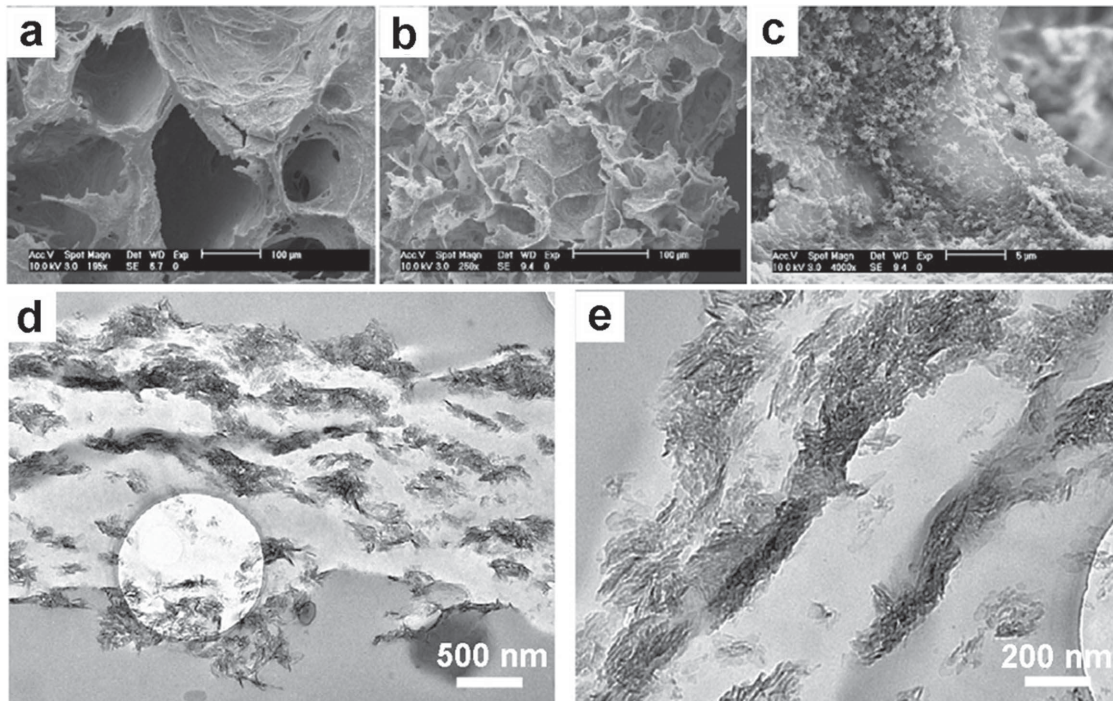


Figure 15. a) SEM image of porous scaffold fabricated by synchronous collagen biomineralization process. b) Post-mineralization of mineralized collagen scaffold in SBF. c) Magnification of panel b). d) TEM image of thin section of three-dimensional mineralized scaffold. e) Magnification of panel d). Reproduced with permission.^[171] Copyright 2008, Elsevier Ltd.

7.2. Dense Liquid Crystalline Collagen Scaffolds

Lamellar bone has a microstructural arrangement, in which adjacent lamellae of parallel fibril arrays have offset directions.^[175] This mesoscale arrangement is due to the cholesteric liquid crystalline order arising from concentrated

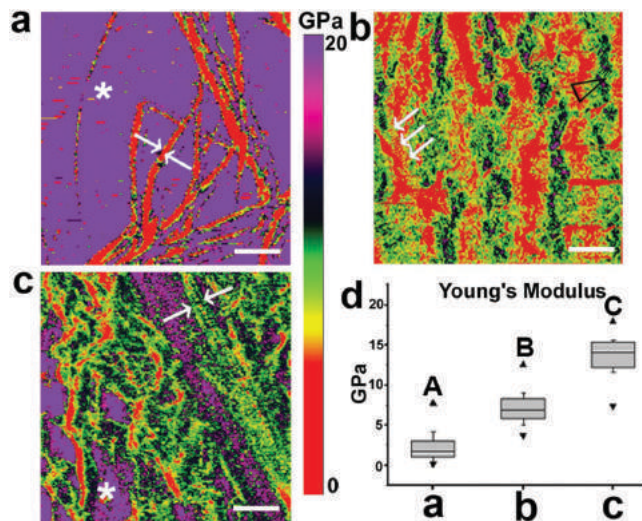


Figure 16. a–c) AFM property maps of the Young's modulus of collagen (a), EMC (b) and IMC (c). d) Box plot of the Young's modulus of collagen (a), EMC (b) and IMC (c). Asterisk: mica base. Arrows: single fibril. Different uppercase letters above each box denote significant differences in the modulus distribution among the three groups. Scale bar = 1 μm . Reproduced with permission.^[93]

collagen solutions. However, most of the current research on collagen self-assembly utilizes dilute type-I collagen (< 3 mg/ml) from bovine and rat tail tendons, and calfskin.^[176–178] It has been shown that densification of dilute tropocollagen solutions could produce various collagen scaffolds with controlled concentration, morphology and homogeneity.^[179–181] Giraud-Guille et al. generated liquid crystalline collagen (LCC) scaffolds by densifying tropocollagen solutions (≈ 90 mg/ml) via ammonia vapor diffusion.^[179,181–183] Considering the cytotoxicity of ammonia, a molecular crowding mechanism based on poly(ethylene glycol) mediated dialysis system is applied to produce biomimetic LCC scaffolds with similar cholesteric order.^[180,184] The nanostructure of LCC observed by TEM exhibited well-aligned fibrils with characteristic D-period. Since mineralized ECM is essential to provide structure and mechanical support for musculoskeletal locomotion, Wingender et al. further mineralized LCC scaffolds by the PILP process and generated a “lamellar” microstructure with chemical compositions and hierarchical organization similar to natural bone (**Figure 18**).^[184] Furthermore, the mineralized LCC showed a high degree of intrafibrillar mineralization with HA crystals co-aligned with the fibril axis. Although previous one-step co-precipitation/fibrillogenesis strategy could produce a macrostructured scaffold, it lacked bone-like hierarchical nanostructure and the overall mineral content was low.^[165–167,184] The successful reproduction of “lamellar” microstructure by mineralized LCC makes us much closer to achieve hierarchically-structured, collagen/CaP nanocomposites, which can serve as load-bearing, porous, biocompatible and biodegradable bone substitutes in TE.

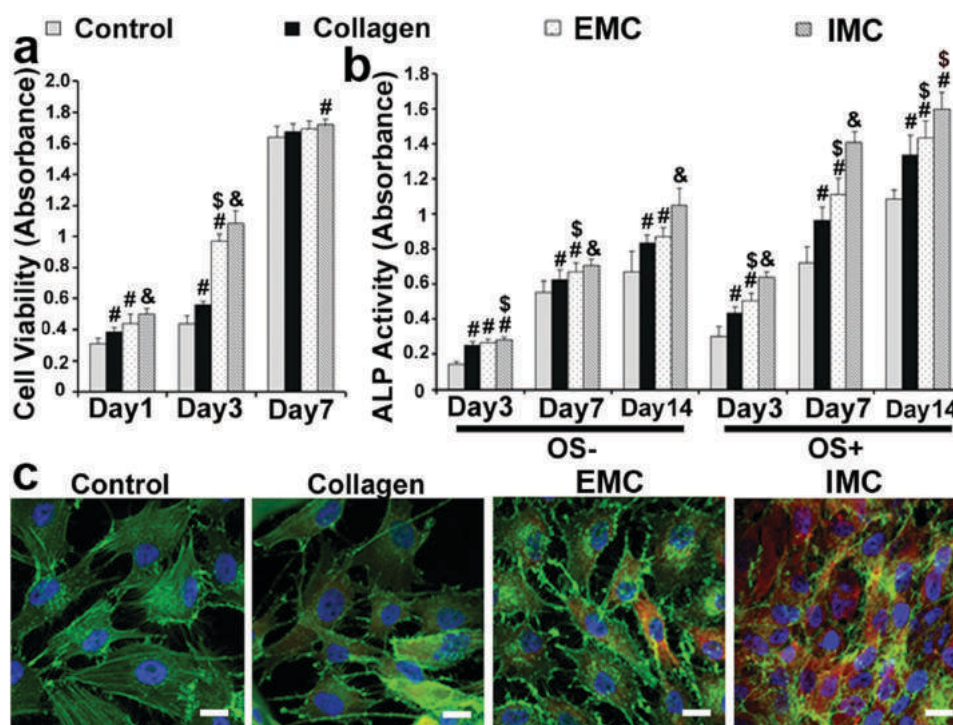


Figure 17. a) Cell viability. b) Alkaline phosphate activity. # = < 0.05 vs. control; \$ = < 0.05 vs. collagen; & = < 0.05 vs. all other groups (ANOVA). c) Confocal microscopy images of cells cultured on different substrates. Green stands for actin filaments, red stands for cell adhesion and blue stands for cell nuclei. Scale bar = 20 μm. Reproduced with permission.^[93]

7.3. Biomimetic Electrospun Collagen Nanofibres

Native bone ECM provides a web of intricate nanofibers to support bone-forming cells.^[185] Synthetic scaffolds with nanofibrous structures would offer larger surface areas to absorb proteins and provide more binding sites for cell-membrane receptors (Figure 19).^[185] Electrospinning is a ubiquitous technique and widely used in TE to fabricate polymeric nanofibers mimicking the ECM geometry. The desirable electrospun collagen nanofibers should be continuous and uniform, and have interconnected pore structure and suitable mechanical property. However, the characteristics of the nanofibers can be influenced by solution properties such as solvent volatility, solution viscosity and conductivity; and processing parameters such as flow rate and strength of electric field.^[186] It has been shown that fluoroalcohols result in conformational change of native proteins,^[187] and electrospun fibers lack typical 67nm cross-banding of native collagen.^[187–190] Although collagenous bone grafts provide greater bioactivity and biocompatibility with bone tissue, thereby favoring tissue regeneration,^[191,192] these biological functions depend on the unique ultrastructural axial periodicity of collagen.^[188]

Electrospun collagen nanofibers present poor mechanical properties and thermal stability, which result in collagen denature during the electrospinning process.^[188,190] Therefore, the incorporation of CaP minerals may improve the stability and mechanical properties of the nanofibers, and finally create more biomimetic constructions. It has been reported that co-spinning of collagen and HA could increase the diameter and surface roughness of the nanofibrous composite.^[189] There was positive correlation between the HA content and

the modulus of the nanofibers. Liao et al. also reported mineralization of pre-fabricated electrospun collagen nanofibers, which lead to bone-like apatite formation over collagen surface.^[193] In vitro studies have shown that the electrospun collagen/HA nanofibers exhibit enhanced biocompatibility and osteogenic potential.^[194,195] Electrospinning is an effective method to produce nanofibers with various parameters, and provides ideal niches for cell growth and differentiation. However, problems such as collagen denaturation and poor biomechanical properties of the fibers should be fully solved in future study.

8. Conclusions and Perspectives

Bone, as a mineralized biomaterial, mainly consists of collagen and HA nanophases arranged in complex hierarchical architectures with characteristic dimensions spanning from the nano- to the macroscale. These complex hierarchical structures possess excellent mechanical properties, combining stiffness and toughness. The precise organization of collagen fibrils and HA nanocrystals at the nanoscale brings nanomechanical heterogeneities, which enable a mechanism of high energy dissipation and resistance to fracture. Enormous progress has been made over the last few decades in understanding the process of bone biomineralization. Some knowledge has been acquired about the role of ACP precursors and organic proteins, such as collagen and NCPs, in achieving a morphologically controlled deposition of mineral as opposed to precipitation of unstructured agglomerates of crystals.

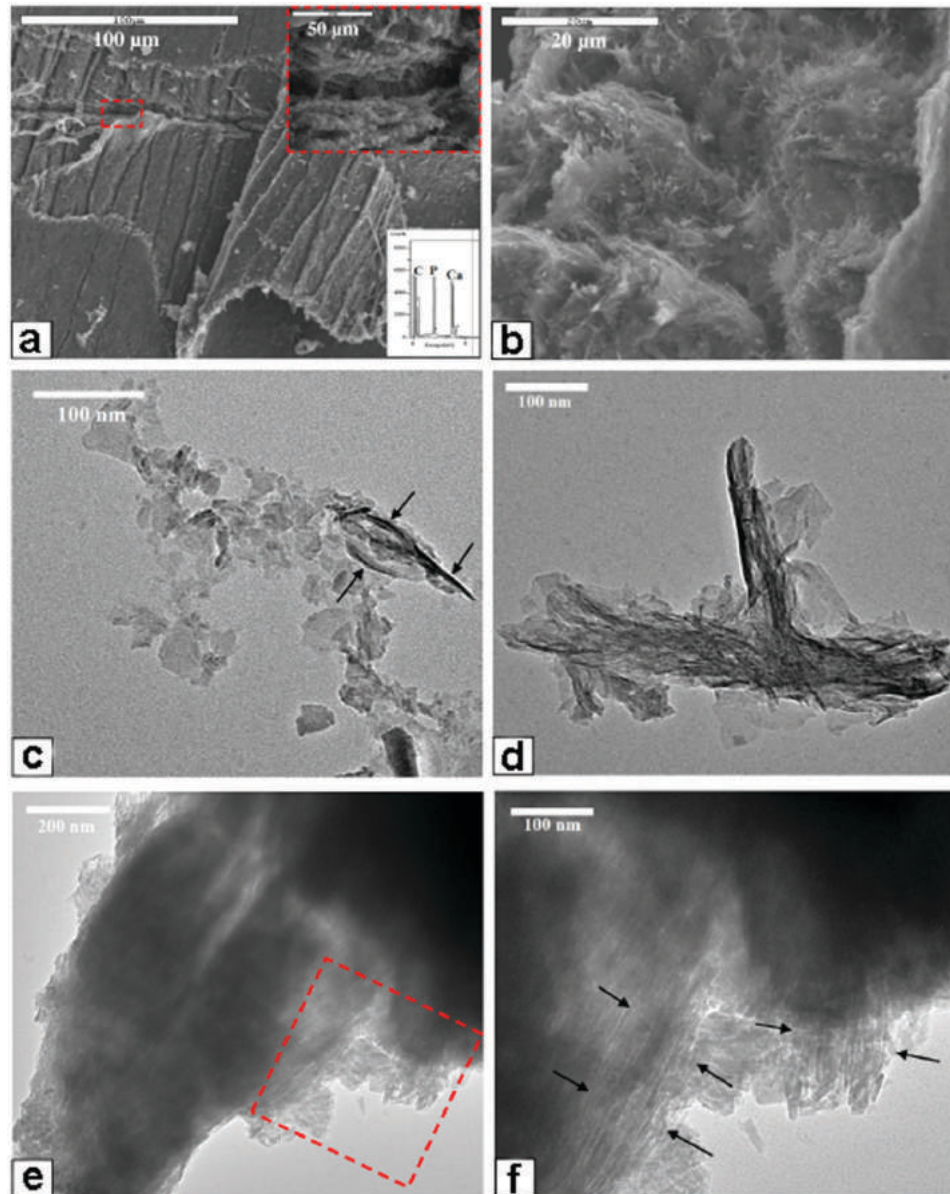


Figure 18. a) SEM micrograph of PILP-mineralized aligned lamella. b) Magnification of the interior lamella in panel a), showing cholesteric organization of the fibrils. c) TEM nanograph of cryo-pulverized mineralized lamella, showing platelet morphology of individual mineral crystals when viewed edge-on. d) TEM nanograph of cryo-pulverized mineralized lamella with almost orthogonal overlapping collagen fibrils. e) TEM nanograph of multiple aligned fibrils, showing 67-nm dark bands. f) Magnification of a thinner edge in panel e), showing the intrafibrillar crystals co-oriented with the fibril axis. Reproduced with permission.^[184] Copyright 2016, Elsevier Ltd.

However, there is still a long way to get a full understanding of bone biomineralization.

Nature's hierarchical design approach confers high strength, toughness and porosity. The excellent mechanical properties derived from a hierarchical nanostructure have inspired chemists and material scientists to develop biomimetic strategies for artificial bone grafts in TE. At the present time, the micro- and nanoscale hierarchical levels of bone (i.e., mineralized collagen) can be reproduced by the biomimetic bottom-up mineralization approach. The bioinspired mineralized collagen scaffolds exhibit enhanced mechanical properties and biofunctions, which are important for a functional, engineered bone tissue. The efficient processing of

hierarchical structures at multiscale levels, and the realization in situ of hard tissue regeneration, remain future goals. It can be anticipated that bioinspired bone TE will dramatically benefit from the multi-level hierarchical structures.

Acknowledgements

Y. L. and D. L. contributed equally to this work. This work was financially supported by the National Science Foundations of China Nos. 81571815 (Y.L.), 21422507 and 21321003 (T.W.), the

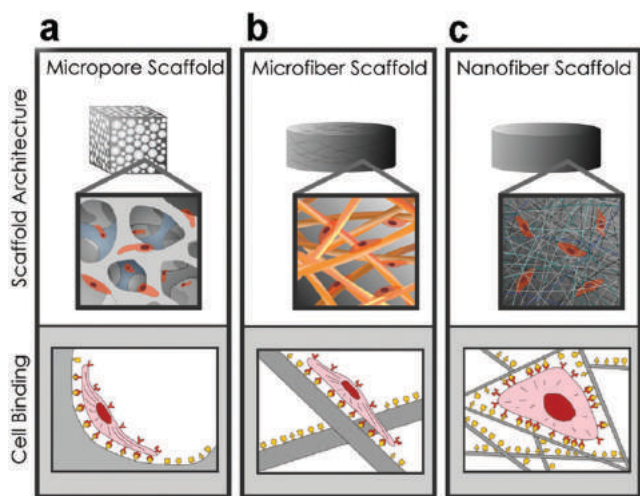


Figure 19. Influences of scaffold structure on cell adhesion and spreading. a,b) Cells adhering to microscale scaffolds spread as if seeded on flat substrates. c) Nanoscale scaffolds provide more binding sites to cell membrane receptors. Reproduced with permission.^[185] Copyright 2005, The American Association for the Advancement of Science.

Science Foundation of China University of Petroleum (Beijing) No. 2462015YJRC009 (D.L.), the PetroChina Innovation Foundation No. 2015D-5006-0401 (D.L.), the Beijing Municipal Natural Science Foundation No. 7152156 (Y.L.) and the 1,000 Young Talents program (T.W.)

[1] U. G. K. Wegst, H. Bai, E. Saiz, A. P. Tomsia, R. O. Ritchie, *Nat. Mater.* **2015**, *14*, 23.
 [2] J. D. Currey, *Science* **2005**, *309*, 253.
 [3] J. Aizenberg, J. C. Weaver, M. S. Thanawala, V. C. Sundar, D. E. Morse, P. Fratzl, *Science* **2005**, *309*, 275.
 [4] N. Reznikov, R. Shahar, S. Weiner, *Bone* **2014**, *59*, 93.
 [5] W. Traub, T. Arad, S. Weiner, *Proc. Natl. Acad. Sci. USA* **1989**, *86*, 9822.
 [6] S. Weiner, H. D. Wagner, *Annu. Rev. Mater. Sci.* **1998**, *28*, 271.
 [7] I. Jager, P. Fratzl, *Biophys. J.* **2000**, *79*, 1737.
 [8] M. J. Glimcher, *Rev. Mineral. Geochem.* **2006**, *64*, 223.
 [9] Y. C. Chai, A. Carlier, J. Bolander, S. J. Roberts, L. Geris, J. Schrooten, H. van Oosterwyck, F. P. Luyten, *Acta. Biomater.* **2012**, *8*, 3876.
 [10] A. L. Boskey, *Connect. Tissue Res.* **1996**, *35*, 357.
 [11] L. C. Palmer, C. J. Newcomb, S. R. Kaltz, E. D. Spoecker, S. I. Stupp, *Chem. Rev.* **2008**, *108*, 4754.
 [12] M. E. Launey, M. J. Buehler, R. O. Ritchie, *Annu. Rev. Mater. Res.* **2010**, *40*, 25.
 [13] N. Reznikov, R. Shahar, S. Weiner, *Acta. Biomater.* **2014**, *10*, 3815.
 [14] F. Z. Cui, Y. Li, J. Ge, *Mat. Sci. Eng. R* **2007**, *57*, 1.
 [15] D. J. Prockop, K. I. Kivirikko, *Annu. Rev. Biochem.* **1995**, *64*, 403.
 [16] A. J. Hodge, J. A. Petruska, *Aspects of protein structure*, Academic Press New York, **1963**, 289.
 [17] A. Veis, *Connect. Tissue Res.* **1982**, *10*, 11.
 [18] K. Gelse, E. Poschl, T. Aigner, *Adv. Drug. Deliver. Rev.* **2003**, *55*, 1531.
 [19] D. Silver, J. Miller, R. Harrison, D. J. Prockop, *Proc. Natl. Acad. Sci. USA* **1992**, *89*, 9860.
 [20] Z. J. Xu, Y. Yang, W. L. Zhao, Z. Q. Wang, W. J. Landis, Q. Cui, N. Sahai, *Biomaterials* **2015**, *39*, 59.

[21] W. Landis, M. Song, A. Leith, L. McEwen, B. McEwen, *J. Struct. Biol.* **1993**, *110*, 39.
 [22] W. J. Landis, R. Jacquet, *Calcif. Tissue Int.* **2013**, *93*, 329.
 [23] F. H. Silver, W. J. Landis, *Connect. Tissue Res.* **2011**, *52*, 242.
 [24] K. M. Meek, J. A. Chapman, R. A. Hardcastle, *J. Biol. Chem.* **1979**, *254*, 710.
 [25] D. B. Wang, J. Ye, S. D. Hudson, K. C. K. Scott, S. Lin-Gibson, *J. Colloid. Interf. Sci.* **2014**, *417*, 244.
 [26] B. L. Langdahl, S. H. Ralston, S. F. A. Grant, E. F. Eriksen, *J. Bone Miner. Res.* **1998**, *13*, 1384.
 [27] V. Mann, E. E. Hobson, B. Li, T. L. Stewart, S. F. Grant, S. P. Robins, R. M. Aspden, S. H. Ralston, *J. Clin. Invest.* **2001**, *107*, 899.
 [28] M. Bernad, M. Martinez, M. Escalona, M. Gonzalez, C. Gonzalez, M. Garces, M. Del Campo, E. M. N. Mola, R. Madero, L. Carreno, *Bone* **2002**, *30*, 223.
 [29] B. Grabner, W. Landis, P. Roschger, S. Rinnerthaler, H. Peterlik, K. Klaushofer, P. Fratzl, *Bone* **2001**, *29*, 453.
 [30] P. Fratzl, H. S. Gupta, E. P. Paschalis, P. Roschger, *J. Mater. Chem.* **2004**, *14*, 2115.
 [31] H. A. Lowenstam, S. Weiner, *On biomineralization*, Oxford University Press, UK **1989**.
 [32] M. J. Olszta, X. Cheng, S. S. Jee, R. Kumar, Y.-Y. Kim, M. J. Kaufman, E. P. Douglas, L. B. Gower, *Mater. Sci. Eng., R* **2007**, *58*, 77.
 [33] J. D. Currey, *Bones: Structure and Mechanics*, Princeton University Press, USA **2002**.
 [34] J. D. Currey, *J. Bone Miner. Res.* **2003**, *18*, 591.
 [35] W. J. Landis, *Connect. Tissue Res.* **1996**, *34*, 239.
 [36] W. J. Landis, K. J. Hodgins, J. Arena, M. J. Song, B. F. McEwen, *Microsc. Res. Tech.* **1996**, *33*, 192.
 [37] P. Fratzl, N. Fratzl-Zelman, K. Klaushofer, *Biophys. J.* **1993**, *64*, 260.
 [38] P. Fratzl, M. Groschner, G. Vogl, H. Plenk, J. Eschberger, N. Fratzl-Zelman, K. Koller, K. Klaushofer, *J. Bone Miner. Res.* **1992**, *7*, 329.
 [39] P. Fratzl, *J. Appl. Crystallogr.* **2003**, *36*, 397.
 [40] O. Paris, I. Zizak, H. Lichtenegger, P. Roschger, K. Klaushofer, P. Fratzl, *Cellular and molecular biology (Noisy-le-Grand, France)* **2000**, *46*, 993.
 [41] E. F. Morgan, G. L. Barnes, T. A. Einhorn, R. Marcus, D. Feldman, D. Nelson, C. Rosen, *The Bone Organ System: Form and Function*. In: R. Marcus, D. Feldman, D. Nelson, C. J. Rosen, eds. *Fundamentals of Osteoporosis*, San Diego, CA: Elsevier Academic Press, **2008**, 1.
 [42] T. Hassenkam, G. E. Fantner, J. A. Cutroni, J. C. Weaver, D. E. Morse, P. K. Hansma, *Bone* **2004**, *35*, 4.
 [43] A. Baig, J. Fox, R. Young, Z. Wang, J. Hsu, W. Higuchi, A. Chhetry, H. Zhuang, M. Otsuka, *Calcif. Tissue Int.* **1999**, *64*, 437.
 [44] A. George, A. Veis, *Chem. Rev.* **2008**, *108*, 4670.
 [45] G. He, T. Dahl, A. Veis, A. George, *Nat. Mater.* **2003**, *2*, 552.
 [46] L. Fisher, D. Torchia, B. Fohr, M. Young, N. Fedarko, *Biochem. Biophys. Res. Co.* **2001**, *280*, 460.
 [47] L. W. Fisher, N. S. Fedarko, *Connect. Tissue Res.* **2003**, *44*, 33.
 [48] S. Stock, *Calcif. Tissue Int.* **2015**, *97*, 262.
 [49] A. S. Deshpande, P.-A. Fang, X. Zhang, T. Jayaraman, C. Sfeir, E. Beniash, *Biomacromolecules* **2011**, *12*, 2933.
 [50] S. Morgan, A. A. Poundarik, D. Vashishth, *Calcif. Tissue Int.* **2015**, *97*, 281.
 [51] O. E. Nikel, D. Laurencin, S. A. McCallum, C. M. Gundberg, D. Vashishth, *Langmuir* **2013**, *29*, 13873.
 [52] H. S. Gupta, W. Wagermaier, G. A. Zickler, D. Raz-Ben Aroush, S. S. Funari, P. Roschger, H. D. Wagner, P. Fratzl, *Nano Lett.* **2005**, *5*, 2108.
 [53] A. A. Poundarik, T. Diab, G. E. Sroga, A. Ural, A. L. Boskey, C. M. Gundberg, D. Vashishth, *Proc. Nat. Acad. Sci. USA* **2012**, *109*, 19178.

- [54] G. E. Fantner, T. Hassenkam, J. H. Kindt, J. C. Weaver, H. Birkedal, L. Pechenik, J. A. Cutroni, G. A. Cidade, G. D. Stucky, D. E. Morse, *Nat. Mater.* **2005**, *4*, 612.
- [55] G. E. Fantner, J. Adams, P. Turner, P. J. Thurner, L. W. Fisher, P. K. Hansma, *Nano Lett.* **2007**, *7*, 2491.
- [56] P. Fantazzini, V. Bortolotti, R. J. Brown, M. Camaiti, C. Garavaglia, R. Viola, G. Giavaresi, *J. Appl. Phys.* **2004**, *95*, 339.
- [57] D. Burr, *Bone* **2002**, *31*, 8.
- [58] E. E. Wilson, A. Awonusi, M. D. Morris, D. H. Kohn, M. M. Tecklenburg, L. W. Beck, *J. Bone Miner. Res.* **2005**, *20*, 625.
- [59] E. E. Wilson, A. Awonusi, M. D. Morris, D. H. Kohn, M. M. Tecklenburg, L. W. Beck, *Biophys. J.* **2006**, *90*, 3722.
- [60] R. K. Rai, N. Sinha, *J. Phys. Chem. C* **2011**, *115*, 14219.
- [61] C. H. Yoder, J. D. Pasteris, K. N. Worcester, D. V. Schermerhorn, *Calcif. Tissue Int.* **2012**, *90*, 60.
- [62] J. R. Dorvee, A. Veis, *J. Struct. Biol.* **2013**, *183*, 278.
- [63] Y. Wang, S. von Euw, F. M. Fernandes, S. Cassaignon, M. Selmane, G. Laurent, G. Pehau-Arnaudet, C. Coelho, L. Bonhomme-Coury, M.-M. Giraud-Guille, *Nat. Mater.* **2013**, *12*, 1144.
- [64] H. Gao, B. Ji, I. L. Jäger, E. Arzt, P. Fratzl, *Proc. Natl. Acad. Sci. USA* **2003**, *100*, 5597.
- [65] P. Fratzl, N. Fratzl-Zelman, K. Klaushofer, G. Vogl, K. Koller, *Calcif. Tissue Int.* **1991**, *48*, 407.
- [66] P. Fratzl, *Nat. Mater.* **2008**, *7*, 610.
- [67] K. J. Koester, J. Ager, R. Ritchie, *Nat. Mater.* **2008**, *7*, 672.
- [68] M. A. Meyers, J. McKittrick, P.-Y. Chen, *Science* **2013**, *339*, 773.
- [69] H. S. Gupta, J. Seto, W. Wagermaier, P. Zaslansky, P. Boescke, P. Fratzl, *Proc. Natl. Acad. Sci. USA* **2006**, *103*, 17741.
- [70] U. Akiva, H. D. Wagner, S. Weiner, *J. Mater. Sci.* **1998**, *33*, 1497.
- [71] H. Gao, *Int. J. Fracture* **2006**, *138*, 101.
- [72] M. J. Buehler, *Nanotechnology* **2007**, *18*, 295102.
- [73] A. K. Nair, A. Gautieri, S.-W. Chang, M. J. Buehler, *Nat. Commun.* **2013**, *4*, 1724.
- [74] Z. Qin, A. Gautieri, A. K. Nair, H. Inbar, M. J. Buehler, *Langmuir* **2012**, *28*, 1982.
- [75] E. Mackie, *Int. J. Biochem. Cell Bio.* **2003**, *35*, 1301.
- [76] D. Cameron, *Clin. Orthop. Relat. Res.* **1963**, *26*, 199.
- [77] E. Bonucci, *Calcification in biological systems*, CRC Press, Boca Raton, USA, **1992**.
- [78] S. V. Dorozhkin, M. Epple, *Angew. Chem. Int. Ed.* **2002**, *41*, 3130.
- [79] S. Weiner, W. Traub, *Organization of crystals in bone. In: Mechanisms and phylogeny of mineralization in biological systems*, Springer, Tokyo, Japan, **1991**, 247.
- [80] M. D. Grynopas, S. Omelon, *Bone* **2007**, *41*, 162.
- [81] S. Weiner, L. Addadi, *Science* **2002**, *298*, 375.
- [82] W. E. Brown, J. P. Smith, J. R. Lehr, A. W. Frazier, *Nature* **1962**, *196*, 1050.
- [83] S. Weiner, W. Traub, *The FASEB journal* **1992**, *6*, 879.
- [84] N. J. Crane, V. Popescu, M. D. Morris, P. Steenhuis, M. A. Ignelzi, *Bone* **2006**, *39*, 434.
- [85] J. Mahamid, A. Sharir, L. Addadi, S. Weiner, *Proc. Natl. Acad. Sci. USA* **2008**, *105*, 12748.
- [86] J. Mahamid, B. Aichmayer, E. Shimoni, R. Ziblat, C. Li, S. Siegel, O. Paris, P. Fratzl, S. Weiner, L. Addadi, *Proc. Natl. Acad. Sci. USA* **2010**, *107*, 6316.
- [87] E. Beniash, R. A. Metzler, R. S. Lam, P. Gilbert, *J. Struct. Biol.* **2009**, *166*, 133.
- [88] L. Addadi, S. Raz, S. Weiner, *Adv. Mater.* **2003**, *15*, 959.
- [89] Y. Politi, T. Arad, E. Klein, S. Weiner, L. Addadi, *Science* **2004**, *306*, 1161.
- [90] Y. Politi, Y. Levi-Kalishman, S. Raz, F. Wilt, L. Addadi, S. Weiner, I. Sagi, *Adv. Funct. Mater.* **2006**, *16*, 1289.
- [91] Y. Liu, Y.-K. Kim, L. Dai, N. Li, S. O. Khan, D. H. Pashley, F. R. Tay, *Biomaterials* **2011**, *32*, 1291.
- [92] Y. Liu, N. Li, Y. P. Qi, L. Dai, T. E. Bryan, J. Mao, D. H. Pashley, F. R. Tay, *Adv. Mater.* **2011**, *23*, 975.
- [93] Y. Liu, D. Luo, X. X. Kou, X. D. Wang, F. R. Tay, Y. L. Sha, Y. H. Gan, Y. H. Zhou, *Adv. Funct. Mater.* **2013**, *23*, 1404.
- [94] F. Nudelman, K. Pieterse, A. George, P. H. Bomans, H. Friedrich, L. J. Brylka, P. A. Hilbers, G. de With, N. A. Sommerdijk, *Nat. Mater.* **2010**, *9*, 1004.
- [95] D. Gebauer, A. Völkel, H. Cölfen, *Science* **2008**, *322*, 1819.
- [96] E. M. Pouget, P. H. Bomans, J. A. Goos, P. M. Frederik, N. A. Sommerdijk, *Science* **2009**, *323*, 1455.
- [97] A. Dey, P. H. Bomans, F. A. Müller, J. Will, P. M. Frederik, G. de With, N. A. Sommerdijk, *Nat. Mater.* **2010**, *9*, 1010.
- [98] H. Cölfen, *Nat. Mater.* **2010**, *9*, 960.
- [99] W. J. Habraken, J. Tao, L. J. Brylka, H. Friedrich, L. Bertinetti, A. S. Schenk, A. Verch, V. Dmitrovic, P. H. Bomans, P. M. Frederik, *Nat. Commun.* **2013**, *4*, 1507.
- [100] G. He, S. Gajjaraman, D. Schultz, D. Cookson, C. Qin, W. T. Butler, J. Hao, A. George, *Biochemistry* **2005**, *44*, 16140.
- [101] G. K. Hunter, H. A. Goldberg, *Biochemical Journal* **1994**, *302*, 175.
- [102] B. Houston, A. J. Stewart, C. Farquharson, *Bone* **2004**, *34*, 629.
- [103] S. Roberts, S. Narisawa, D. Harmey, J. L. Millán, C. Farquharson, *J. Bone Miner. Res.* **2007**, *22*, 617.
- [104] F. A. Saad, E. Salih, M. J. Glimcher, *J. Cell. Biochem.* **2008**, *103*, 852.
- [105] B. Grohe, J. O'Young, D. A. Ionescu, G. Lajoie, K. A. Rogers, M. Karttunen, H. A. Goldberg, G. K. Hunter, *J. Am. Chem. Soc.* **2007**, *129*, 14946.
- [106] A. L. Arsenault, *Bone and Mineral* **1989**, *6*, 165.
- [107] L. Siperko, W. Landis, *J. Struct. Biol.* **2001**, *135*, 313.
- [108] B. E. Alexander, T. L. Daulton, G. M. Genin, J. D. Pasteris, B. Wopenka, S. Thomopoulos, In: *The nano-physiology of mineralized tissues*, ASME 2009 Summer Bioengineering Conference, American Society of Mechanical Engineers: **2009**, 55.
- [109] B. Alexander, T. L. Daulton, G. M. Genin, J. Lipner, J. D. Pasteris, B. Wopenka, S. Thomopoulos, *J. R. Soc. Interface* **2012**, *9*, 1774.
- [110] M. Glimcher, *Biomaterials* **1990**, *11*, 7.
- [111] A. Veis, *Rev. Mineral. Geochem.* **2003**, *54*, 249.
- [112] T. Tsuji, K. Onuma, A. Yamamoto, M. Iijima, K. Shiba, *Proc. Natl. Acad. Sci. USA* **2008**, *105*, 16866.
- [113] J. A. Chapman, M. Tzaphlidou, K. M. Meek, K. E. Kadler, *Electron Microscopy Reviews* **1990**, *3*, 143.
- [114] D. Christiansen, F. Silver, *Biomimetics* **1992**, *1*, 265.
- [115] D. Christiansen, F. Silver, L. Addadi, *Cells and Materials* **1993**, *3*, 17.
- [116] Y. Wang, T. Azais, M. Robin, A. Vallée, C. Catania, P. Legriell, G. Pehau-Arnaudet, F. Babonneau, M.-M. Giraud-Guille, N. Nassif, *Nat. Mater.* **2012**, *11*, 724.
- [117] L. B. Gower, *Chem. Rev.* **2008**, *108*, 4551.
- [118] D. Toroian, J. E. Lim, P. A. Price, *J. Biol. Chem.* **2007**, *282*, 22437.
- [119] P. A. Price, D. Toroian, J. E. Lim, *J. Biol. Chem.* **2009**, *284*, 17092.
- [120] R. J. Midura, A. Wang, D. Lovitch, D. Law, K. Powell, J. P. Gorski, *J. Biol. Chem.* **2004**, *279*, 25464.
- [121] C. E. Tye, K. R. Rattray, K. J. Warner, J. A. Gordon, J. Sodek, G. K. Hunter, H. A. Goldberg, *J. Biol. Chem.* **2003**, *278*, 7949.
- [122] L. Chen, R. Jacquet, E. Lowder, W. J. Landis, *Bone* **2015**, *71*, 7.
- [123] D. Lickorish, J. A. Ramshaw, J. A. Werkmeister, V. Glattauer, C. R. Howlett, *J. Biomed. Mater. Res. A* **2004**, *68*, 19.
- [124] S. Liao, F. Watari, M. Uo, S. Ohkawa, K. Tamura, W. Wang, F. Cui, *J. Biomed. Mater. Res. B* **2005**, *74*, 817.
- [125] Y. Zhai, F. Cui, Y. Wang, *Curr. Appl. Phys.* **2005**, *5*, 429.
- [126] L. Silverman, A. Boskey, *Calcif. Tissue Int.* **2004**, *75*, 494.
- [127] A.-W. Xu, Y. Ma, H. Cölfen, *J. Mater. Chem.* **2007**, *17*, 415.
- [128] S. Wohlrab, N. Pinna, M. Antonietti, H. Cölfen, *Chem.-Eur. J.* **2005**, *11*, 2903.
- [129] M. Niederberger, H. Cölfen, *Phys. Chem. Chem. Phys.* **2006**, *8*, 3271.

- [130] W. Zhang, S. Liao, F. Cui, *Chem. Mater.* **2003**, *15*, 3221.
- [131] J. Goes, S. Figueiro, A. Oliveira, A. Macedo, C. Silva, N. Ricardo, A. Sombra, *Acta Biomater.* **2007**, *3*, 773.
- [132] W. Traub, T. Arad, S. Weiner, *Matrix* **1992**, *12*, 251.
- [133] R. J. DeVolder, I. W. Kim, E.-S. Kim, H. Kong, *Tissue Eng. Part A* **2012**, *18*, 1642.
- [134] M. Gudur, R. R. Rao, Y.-S. Hsiao, A. W. Peterson, C. X. Deng, J. P. Stegemann, *Tissue Eng. Part C* **2012**, *18*, 935.
- [135] L. Dai, Y.-P. Qi, L.-N. Niu, Y. Liu, C. R. Pucci, S. W. Looney, J.-Q. Ling, D. H. Pashley, F. R. Tay, *Cryst. Growth Des.* **2011**, *11*, 3504.
- [136] F. C. Meldrum, H. Cölfen, *Chem. Rev.* **2008**, *108*, 4332.
- [137] L. B. Gower, D. J. Odom, *J. Cryst. Growth* **2000**, *210*, 719.
- [138] N. Gehrke, N. Nassif, N. Pinna, M. Antonietti, H. S. Gupta, H. Cölfen, *Chem. Mater.* **2005**, *17*, 6514.
- [139] D. Volkmer, M. Harms, L. Gower, A. Ziegler, *Angew. Chem. Int. Ed.* **2005**, *44*, 639.
- [140] M. Olszta, E. Douglas, L. Gower, *Calcif. Tissue Int.* **2003**, *72*, 583.
- [141] M. J. Olszta, D. J. Odom, E. P. Douglas, L. B. Gower, *Connect. Tissue Res.* **2003**, *44*, 326.
- [142] S. S. Jee, L. Culver, Y. Li, E. P. Douglas, L. B. Gower, *J. Cryst. Growth* **2010**, *312*, 1249.
- [143] S.-S. Jee, T. T. Thula, L. B. Gower, *Acta Biomater.* **2010**, *6*, 3676.
- [144] D. E. Rodriguez, T. Thula-Mata, E. J. Toro, Y.-W. Yeh, C. Holt, L. S. Holliday, L. B. Gower, *Acta Biomater.* **2014**, *10*, 494.
- [145] S. Gajjeraman, K. Narayanan, J. Hao, C. Qin, A. George, *J. Biol. Chem.* **2007**, *282*, 1193.
- [146] S. Weiner, *J. Struct. Biol.* **2008**, *163*, 229.
- [147] Y. K. Kim, L.-S. Gu, T. E. Bryan, J. R. Kim, L. Chen, Y. Liu, J. C. Yoon, L. Breschi, D. H. Pashley, F. R. Tay, *Biomaterials* **2010**, *31*, 6618.
- [148] L.-S. Gu, Y. K. Kim, Y. Liu, K. Takahashi, S. Arun, C. E. Wimmer, R. Osorio, J.-Q. Ling, S. W. Looney, D. H. Pashley, *Acta Biomater.* **2011**, *7*, 268.
- [149] T. T. Thula, D. E. Rodriguez, M. H. Lee, L. Pendi, J. Podschun, L. B. Gower, *Acta Biomater.* **2011**, *7*, 3158.
- [150] A. S. Deshpande, E. Beniash, *Cryst. Growth Des.* **2008**, *8*, 3084.
- [151] W. E. Müller, X. Wang, F.-Z. Cui, K. P. Jochum, W. Tremel, J. Bill, H. C. Schröder, F. Natalio, U. Schloßmacher, M. Wiens, *Appl. Microbiol. Biot.* **2009**, *83*, 397.
- [152] H. Cölfen, *Angew. Chem. Int. Ed.* **2008**, *47*, 2351.
- [153] S. Svenson, D. A. Tomalia, *Adv. Drug Deliv. Rev.* **2005**, *57*, 2106.
- [154] S. J. Yan, Z. H. Zhou, F. Zhang, S. P. Yang, L. Z. Yang, X. B. Yu, *Mater. Chem. Phys.* **2006**, *99*, 164.
- [155] L. Xie, L. Wang, X. Jia, G. Kuang, S. Yang, H. Feng, *Polym. Bull.* **2011**, *66*, 119.
- [156] S. Yang, H. He, L. Wang, X. Jia, H. Feng, *Chem. Commun.* **2011**, *47*, 10100.
- [157] D. Wu, J. Yang, J. Li, L. Chen, B. Tang, X. Chen, W. Wu, J. Li, *Biomaterials* **2013**, *34*, 5036.
- [158] J. H. Li, J. Yang, J. Y. Li, L. Chen, K. Liang, W. Wu, X. Chen, J. S. Li, *Biomaterials* **2013**, *34*, 6738.
- [159] J. Xin, T. Chen, Z. Lin, P. Dong, H. Tan, J. Li, *Chem. Commun.* **2014**, *50*, 6491.
- [160] R. Langer, D. A. Tirrell, *Nature* **2004**, *428*, 487.
- [161] R. R. Betz, *Orthopedics* **2002**, *25*, S561.
- [162] W. L. Grayson, M. Fröhlich, K. Yeager, S. Bhumiratana, M. E. Chan, C. Cannizzaro, L. Q. Wan, X. S. Liu, X. E. Guo, G. Vunjak-Novakovic, *Proc. Natl. Acad. Sci. USA* **2010**, *107*, 3299.
- [163] J. D. Conway, *Orthop. Clin. North. Am.* **2010**, *41*, 75.
- [164] M. A. Woodruff, C. Lange, J. Reichert, A. Berner, F. Chen, P. Fratzl, J.-T. Schantz, D. W. Huttmacher, *Materials Today* **2012**, *15*, 430.
- [165] J. H. Bradt, M. Mertig, A. Teresiak, W. Pompe, *Chem. Mater.* **1999**, *11*, 2694.
- [166] W. Zhang, S. S. Liao, F. Z. Cui, *Chem. Mater.* **2003**, *15*, 3221.
- [167] S. Liao, F. Watari, M. Uo, S. Ohkawa, K. Tamura, W. Wang, F. Z. Cui, *J. Biomed. Mater. Res. B* **2005**, *74B*, 817.
- [168] R. Burth, M. Gelinsky, W. Pompe, *Tech. Textile* **1999**, *8*, 20.
- [169] A. Bernhardt, A. Lode, S. Boxberger, W. Pompe, M. Gelinsky, *J. Mater. Sci. Mater. Med.* **2008**, *19*, 26.
- [170] H. Domaschke, M. Gelinsky, B. Burmeister, R. Fleig, Th. Hanke, A. Reinstorf, W. Pompe, A. Rosen-Wolff, *Tissue Eng.* **2006**, *12*, 949.
- [171] M. Gelinsky, P. B. Welzel, P. Simon, A. Bernhardt, U. König, *Chem. Eng. J.* **2008**, *137*, 84.
- [172] C. M. Murphy, M. G. Haugh, F. J. O'Brien, *Biomaterials* **2010**, *31*, 461.
- [173] P. Fratzl, H. S. Gupta, E. P. Paschalis, P. Roschger, *J. Mater. Chem.* **2004**, *14*, 2115.
- [174] Y. Liu, D. Luo, S. Liu, Y. Fu, X. Kou, X. Wang, Y. Sha, Y. Gan, Y. Zhou, *J. Biomed. Nanotechnol.* **2014**, *10*, 1049.
- [175] M. M. Giraud-Guille, *Calcif. Tissue Int.* **1988**, *42*, 167.
- [176] K. E. Kadler, D. F. Holmes, J. A. Trotter, J. A. Chapman, *Biochem. J.* **1996**, *316*, 1.
- [177] G. Chandrakasan, D. A. Torchia, K. A. Piez, *J. Biol. Chem.* **1976**, *251*, 6062.
- [178] J. Gross, J. H. Highberger, F. O. Schmitt, *Proc. Natl. Acad. Sci. USA* **1955**, *41*, 1.
- [179] Y. Wang, J. Silvent, M. Robin, F. Babonneau, A. Meddahi-Pelle, N. Nassif, M. M. Giraud-Guille, *Soft Matter* **2011**, *7*, 9659.
- [180] N. Saeidi, K. P. Karmelek, J. A. Paten, R. Zareian, E. DiMasi, J. W. Ruberti, *Biomaterials* **2012**, *33*, 7366.
- [181] M. M. Giraud-Guille, G. Mosser, E. Belamie, *Curr. Opin. Colloid Interface Sci.* **2008**, *13*, 303.
- [182] F. Gobeaux, G. Mosser, A. Anglo, P. Panine, P. Davidson, M. M. Giraud-Guille, E. Belamie, *J. Mol. Biol.* **2008**, *376*, 1509.
- [183] F. Gobeaux, E. Belamie, G. Mosser, P. Davidson, P. Panine, M. M. Giraud-Guille, *Langmuir* **2007**, *23*, 6411.
- [184] B. Wingender, P. Bradley, N. Saxena, J. W. Ruberti, L. Gower, *Matrix Biol.* **2016**, *52*, 384.
- [185] M. M. Stevens, J. H. George, *Science* **2005**, *310*, 1135.
- [186] M. Bognitzki, W. Czado, T. Frese, A. Schaper, M. Hellwig, M. Steinhart, A. Greiner, J. H. Wendorff, *Adv. Mater.* **2001**, *13*, 70.
- [187] K. Gast, A. Siemer, D. Zirwer, G. Damaschun, *Eur. Biophys. J. Biophys.* **2001**, *30*, 273.
- [188] D. I. Zeugolis, S. T. Khew, E. S. Y. Yew, A. K. Ekaputra, Y. W. Tong, L. Y. L. Yung, D. W. Huttmacher, C. Sheppard, M. Raghunath, *Biomaterials* **2008**, *29*, 2293.
- [189] V. Thomas, D. R. Dean, M. V. Jose, B. Mathew, S. Chowdhury, Y. K. Vohra, *Biomacromolecules* **2007**, *8*, 631.
- [190] L. Yang, C. F. C. Fitie, K. O. van der Werf, M. L. Bennink, P. J. Dijkstra, J. Feijen, *Biomaterials* **2008**, *29*, 955.
- [191] S.-W. Tsai, H.-M. Liou, C.-J. Lin, K.-L. Kuo, Y.-S. Hung, R.-C. Weng, F.-Y. Hsu, *PLoS One* **2012**, *7*, 31200.
- [192] A. Aravamudhan, D. M. Ramos, J. Nip, M. D. Harmon, R. James, M. Deng, C. T. Laurencin, X. Yu, S. G. Kumbar, *J. Biomed. Nanotechnol.* **2013**, *9*, 719.
- [193] S. Liao, R. Murugan, C. K. Chan, S. Ramakrishna, *J. Mech. Behav. Biomed. Mater.* **2008**, *1*, 252.
- [194] L. S. Sefcik, R. A. Neal, S. N. Kaszuba, A. M. Parker, A. J. Katz, R. C. Ogle, E. A. Botchwey, *J. Tissue Eng. Regen. Med.* **2008**, *2*, 210.
- [195] M. D. Schofer, U. Boudriot, C. Wack, I. Leifeld, C. Grabedunkel, R. Dersch, M. Rudisile, J. H. Wendorff, A. Greiner, J. R. J. Paletta, S. Fuchs-Winkelmann, *J. Mater. Sci. Mater. Med.* **2009**, *20*, 767.

Received: February 24, 2016

Revised: April 4, 2016

Published online: